12

MICROSCOPIC PLASMA PROCESSES IN THE JOVIAN MAGNETOSPHERE

Richard Mansergh Thorne

Plasma waves observed near Jupiter exhibit characteristics similar to waves in the terrestrial magnetosphere and a quantitative analysis suggests a universality of the generation mechanisms. Electromagnetic whistler-mode waves are enhanced within the high-density plasma torus surrounding the orbit of Io and evidence for electron stable trapping is found in the inner torus. The observed intensity of low-frequency hiss is sufficient to scatter resonant ($\gtrsim$ 100 keV) electrons and cause continuous precipitation loss to the atmosphere at a rate comparable to 5% of the limit imposed by strong pitch-angle diffusion. The energy flux into the Jovian atmosphere is estimated to be approximately 3 mW/m^2 over a broad invariant latitude range $65° \lesssim \Lambda \lesssim 70°$ mapping from the Io torus. Total power dissipation may therefore approach 10^{13} W. But because the energetic electron deposition occurs deep in the Jovian atmosphere, little of the concomitant auroral emission should be detectable by Voyager. The intermittent bursts of electromagnetic chorus and the equatorially confined electrostatic $(n + 1/2)\, f_{c.e}$ waves can at times scatter lower energy (keV) electrons on strong diffusion. The net energy deposition, however, is typically less than 0.5 mW/m^2 and the total power dissipation over the entire auroral zone should be $\lesssim 10^{12}$ W. Energetic ions exhibit evidence for rapid precipitation loss throughout the plasma torus. Although the waves responsible for such scattering have not yet been identified, ion precipitation loss near the strong diffusion limit apparently offers the only viable mechanism to excite the observed auroral emissions. Over the reported energy range ($E_p \gtrsim 500$ keV) the anticipated power dissipation can exceed 2×10^{13} W, but an extrapolation down to ion energies comparable to 100 keV could increase this to 10^{14} W, which is comparable to the auroral requirements.

It is unlikely that the solar wind plays a significant role in the energetics of the Jovian magnetosphere. The most viable power supply for the intense auroral dissipation is the rotational energy of Jupiter. If the mechanism for tapping this energy is mass loading in the torus, the observed auroral emissions require an injection rate of heavy thermal ions from Io in excess of 10^{29}/s. The anticipated precipitation of energetic ions into the Jovian atmosphere can also produce a significant flux of suprathermal (> 20 eV) secondary electrons. If the precipitation is dominated by energetic ($\gtrsim 100$ keV) heavy ions, the energy flux of escaping secondary electrons could provide a heat source ($\gtrsim 10^{12}$ W) to the torus comparable to the observed radiative cooling and the ambipolar outflow could inject cold hydrogen ions into the magnetosphere at a rate comparable to heavy ion injection from Io.

12.1. Introduction

Despite the acknowledged success of the macroscopic (MHD) description of planetary magnetospheres, there are many fundamental plasma phenomena that can be understood only through a detailed treatment of the microscopic plasma processes. Resonant wave-particle interactions, during which energy can be efficiently transferred between the energetic particle population and plasma waves, have been demonstrated to be of paramount importance in the Earth's magnetosphere [e.g., Andronov and Trakhtengerts, 1964; Kennel and Petschek, 1966; Cornwall, 1966; Cornwall, Coroniti, and Thorne, 1970; Lyons, Thorne, and Kennel, 1972; Thorne, 1976] and for a number of years it has been conjectured that similar processes should occur at Jupiter [Thorne

and Coroniti, 1972; Kennel, 1972; Coroniti, 1974; Coroniti, Kennel, and Thorne, 1974; Baker and Goertz, 1976; Barbosa and Coroniti, 1976; Fillius et al., 1976; Scarf, 1976; Scarf and Sanders, 1976; Sentman and Goertz, 1978]. Although the adiabatic invariants provide a useful kinematical framework, a strictly adiabatic description of the particle dynamics is inappropriate because the particle distribution function can be radically modified during the interaction with plasma waves. When the waves are reasonably intense, the concomitant wave-particle scattering can be far more effective than collisional processes in causing the injection, acceleration, nonadiabatic transport and ultimate loss of particles from the radiation belts. The in situ particle and field data obtained from Voyager 1 and 2 permit the first quantitative assessment to be made of the importance of such wave-particle interactions in the Jovian magnetosphere.

A detailed review of the plasma waves observed in the Jovian magnetosphere [Scarf, Gurnett, and Kurth, 1979] is given in Chapter 8 together with a brief description of potential mechanisms for wave generation. The remarkable similarity to waves observed in the terrestrial magnetosphere suggests that the knowledge gained from the extensive study of wave-particle processes in the Earth's magnetosphere can be directly applied to Jupiter. It is therefore appropriate to first briefly review the concepts and implications of quasilinear scattering of trapped particles during resonant interactions with various plasma waves with emphasis placed on understanding the mechanisms for wave origin and establishing the rate of particle removal due to pitch-angle scattering loss to the atmosphere. The finite geometrical size of the atmospheric loss-cone places an absolute upper limit on the rate of particle removal. This is attained under strong pitch-angle diffusion [e.g., Kennel, 1969] when particles are scattered across the loss-cone within a bounce period. Estimates are presented for the amplitude of plasma waves required for strong diffusion and these are subsequently compared with Voyager wave observations.

Although the Voyager instrumentation was unable to resolve particle fluxes within the loss-cone, estimates of the precipitation flux can be obtained from the theoretically predicted scattering lifetimes and observations of the trapped particle populations. The particle lifetimes presented here admittedly reflect the author's personal bias and in certain instances have a weak observational basis. Nevertheless, a direct comparison of the theoretically predicted precipitation flux with that required to excite the intense H and H_2 auroral emissions observed in the Jovian polar regions [Broadfoot et al., 1979; Sandel et al., 1979] provides a stringent test on our current ability to adequately model the microscopic plasma processes.

The rapid particle loss from the Jovian magnetosphere places stringent limits on the transport mechanisms for energetic plasma and the ultimate energy source available for intense auroral dissipation. One can also anticipate a strong coupling, both in terms of electrodynamics and particle sources, between the Jovian upper atmosphere and the magnetosphere. Our discussion of such processes, although speculative, is intended as an initial attempt to provide an holistic description of the Jovian plasma physics.

12.2. Wave–particle interactions in the terrestrial magnetosphere

Under adiabatic conditions, the kinematics of energetic radiation belt particles can be uniquely described by the magnetic field topology and the conservation of three adiabatic invariants (μ, J, Φ) associated with basic periodicities in the particle motion [e.g., Northrop, 1963]. Violation of the invariants, however, can occur when the charged particles are subject to a force field fluctuating on a timescale comparable to or faster than that of the respective periodic motion. For the first two invariants this requires a

fluctuating field with characteristic frequencies near $\omega \gtrsim \omega_c ; \tau_b^{-1}$ respectively, where ω_c is the particle cyclotron frequency and τ_b the bounce time for travel between magnetic mirror points. Violation of either invariant leads to pitch-angle scattering and an ultimate loss of trapped particles to the atmosphere. In contrast, violation of the third invariant, which involves fluctuations on a timescale less than the azimuthal drift time τ_d results in nonadiabatic radial transport, which can act either as a source or sink for radiation belt particles.

In the Earth's magnetosphere, fluctuating plasma waves occur spanning the entire range of frequencies required for violation of each invariant, and numerous estimates have been made of the effect of specific wave modes on the trapped particle population. The waves can be grouped into two broad categories, electromagnetic or electrostatic, depending on whether or not there is a measurable fluctuating magnetic field. A detailed review of the principal wave modes observed in the Earth's magnetosphere has recently been provided by Shawhan [1979] and the properties of similar waves detected by Voyager in the Jovian magnetosphere are discussed by Gurnett and Scarf in Chapter 8 of this volume.

In general, the temporal evolution of the radiation-belt environment can be described in terms of a phase-averaged distribution function $f_o(\mu,J,\Phi,t)$ in which nonadiabatic processes are treated as a diffusion with respect to the three adiabatic invariants. The basic form of the multi-dimensional diffusion equation can be written as [e.g., Schulz and Lanzerotti, 1974]

$$\frac{\partial f_o}{\partial t} = \sum_{i,j} \frac{\partial}{\partial J_i} \left(D_{ij} \frac{\partial f_o}{\partial J_j} \right) + S - L \tag{12.1}$$

where J_i are the action integrals associated with the adiabatic periodicities of the motion, D_{ij} are diffusion coefficients and S and L are source and loss terms that are introduced to account for processes that inject or remove particles. Although, in general, all three invariants can be subject to simultaneous violation, it is conceptually convenient to distinguish between velocity space diffusion (in which μ, J are not conserved) and radial diffusion (which violates Φ). Because of the rapid timescales involved in μ, J violation, it is often appropriate to assume that Φ is ostensibly constant and simply treat the diffusion in particle pitch-angle and energy. This approach is taken here to evaluate the role of wave-particle interactions in the scattering loss for trapped particles. The complementary approach of explicitly treating violation of Φ through the radial diffusion equation

$$\frac{\partial f_o}{\partial t} = L^2 \frac{\partial}{\partial L} \frac{D_{LL}}{L^2} \frac{\partial f_o}{\partial L} + S - L \tag{12.2}$$

in which μ or J violation is parameterized by an effective loss term $L \approx f_o/\tau_L$, has been discussed in Chapters 10 and 11 of this volume. We shall also utilize (12.2) in Section 12.3 to establish whether radial diffusion can act as a viable source for energetic particles capable of exciting high-frequency instabilities in the Jovian magnetosphere.

Quasilinear scattering by plasma waves

The scattering of geomagnetically trapped particles by plasma waves is dominated by resonant interactions at harmonics of the particle bounce and cyclotron frequency. However, because emphasis here is placed on processes that lead to a precipitation of particles into the atmosphere, bounce resonance is not specifically treated because

it is usually important only for particles mirroring near the geomagnetic equator [e.g., Roberts and Schulz, 1968]. Scattering into the atmospheric loss cone is predominantly controlled by plasma waves that are Doppler shifted in frequency to some integral multiple ℓ of the particle cyclotron frequency

$$\omega - k_\parallel v_\parallel = \frac{\ell \omega_c}{\gamma} \tag{12.3}$$

where $k_\parallel$, $v_\parallel$ are components of the wave propagation vector and particle velocity along the ambient magnetic field direction and $\gamma = (1 - v^2/c^2)^{-1/2}$. During the interaction, resonant particles are constrained to diffuse in velocity space along surfaces [Kennel and Englemann, 1966] such that

$$(v_\parallel - \omega/k_\parallel)^2 + v_\perp^2 = \text{constant} \tag{12.4}$$

The Landau ($\ell = 0$) resonance thus simply involves energy transfer between the wave and the particle velocity parallel to $\bar{B}$. For the cyclotron ($\ell \neq 0$) resonances, diffusion occurs predominantly in pitch-angle ($v \approx$ constant) for high-energy resonant particles but significant energy diffusion also occurs when the particle velocity becomes comparable to the wave phase speed. However, near the edge of the loss-cone ($v_\perp / v_\parallel << 1$), cyclotron resonant interactions result in essentially pure pitch-angle diffusion for all resonant particles.

The rate of diffusion in velocity space depends sensitively on the resonant wave-mode and the distribution of the fluctuating power spectral density $P(\omega, \bar{k})$ as a function of frequency and wave normal. For the idealized case of pure pitch-angle diffusion, (12.1) can be rewritten in the form

$$\frac{\partial f_o}{\partial t} = \frac{1}{\sin \alpha} \frac{\partial}{\partial \alpha} \sin \alpha \sum_\ell \left(D_{\alpha\alpha}^{(\ell)} \frac{\partial f_o}{\partial \alpha} \right) + S - L \tag{12.5}$$

where $\alpha = \arctan (v_\perp / v_\parallel)$ is the instantaneous pitch-angle and $D_{\alpha\alpha}^{(\ell)} = \langle \Delta\alpha \rangle^2 / 2\Delta t$ is the pitch-angle diffusion coefficient associated with each cyclotron harmonic resonance for a prescribed band of waves. Landau resonant diffusion, although strictly confined to diffusion in $v_\parallel$, can also be included within the above formalism by defining an effective rate of pitch-angle scattering [Roberts and Schulz, 1968; Lyons, Thorne, and Kennel, 1972].

Equation (12.5) prescribes the effect of diffusion at one point in space. To evaluate the time-averaged evolution of the particle distribution function it is first necessary to identify all particles by their equatorial pitch-angle α_o and then average (12.5) over the bounce trajectory between magnetic mirror points to obtain [Lyons, Thorne, and Kennel, 1972]

$$\frac{\partial f_o}{\partial t} = \frac{1}{\mathrm{T}(\alpha_o) \sin 2\alpha_o} \frac{\partial}{\partial \alpha_o} \mathscr{D}_\alpha (\alpha_o)\, T(\alpha_o) \sin 2\alpha_o \frac{\partial f_o}{\partial \alpha_o} + \langle S \rangle - \langle L \rangle \tag{12.6}$$

where $\mathscr{D}_\alpha (\alpha_o)$ is the net bounce averaged effective diffusion coefficient, $\langle S \rangle$ and $\langle L \rangle$ are average source and loss functions, and $T(\alpha_o) \approx 1.38 - 0.64 \sin^{3/4} \alpha_o$ represents the dependence of the particle bounce period on equatorial pitch-angle [Davidson, 1976].

Under conditions when the particle source is negligible ($\langle S \rangle \rightarrow 0$) and losses are due to collisions with the atmosphere, $L(\alpha_o) \sim f_o(\alpha_o)/\tau_L(\alpha_o)$, one can solve (12.6) simultaneously [Spjeldvik and Thorne, 1975] for the precipitation lifetime

$$\frac{1}{\tau_P(E,L)} = \left\langle \frac{1}{\tau_L(E,L,\alpha_o)} \right\rangle \tag{12.7}$$

$$= \frac{\int_o^{\pi/2} \frac{1}{\tau_L(E,L,\alpha_o)} f_o(E,L,\alpha_o) T(\alpha_o) \sin 2\alpha_o \, d\alpha_o}{\int_o^{\pi/2} f_o(E,L,\alpha_o) T(\alpha_o) \sin 2\alpha_o \, d\alpha_o}$$

and the equilibrium pitch-angle distribution

$$f_o(E,L,\alpha_o) = f_o\left(E,L,\frac{\pi}{2}\right) - \int_o^{\pi/2} \frac{d\alpha'_o}{\mathscr{D}_\alpha(E,L,\alpha'_o) T(\alpha'_o) \sin 2\alpha'_o} \tag{12.8}$$

$$\times \int_{\alpha_o^1}^{\pi/2} \left(\frac{1}{\tau_P(E,L)} - \frac{1}{\tau_L(E,L,\alpha''_o)} \right) f_o(E,L,\alpha''_o) T(\alpha''_o) \sin 2\alpha''_o \, d\alpha''_o$$

Alternatively, if the source strength is prescribed, a steady state solution ($\partial f_o/\partial t \rightarrow 0$) to (12.6) can be obtained by equating the rate of injection to the diffusion flux into the loss cone [e.g., Kennel and Petschek, 1966].

In the limit of weak pitch-angle diffusion, $\mathscr{D}_\alpha(\alpha_L) << \alpha_L^2/\tau_b$ when particles are unable to diffuse significantly across the loss-cone α_L within a bounce time τ_b the precipitation lifetime $\tau_P \approx 1/\mathscr{D}_\alpha(\alpha_L)$ and the particle flux exhibits a steep gradient at the edge of the loss-cone. At the opposite extreme under strong diffusion (when $\mathscr{D}_\alpha(\alpha_L) >> \alpha_L^2/\tau_b$) particles can readily diffuse across the dimensions of the loss-cone within a bounce period; the particle flux approaches isotropy, and the bounce averaged precipitation time [Lyons, 1973] approaches an asymptotic limiting value, controlled only by the particle bounce time and the geometric size of the loss cone $\alpha_L^2 = B/B_A \approx 1/2\,L^3$ (for $L >> 1$),

$$\tau_{SD} = \tau_b/3\alpha_L^2 \approx 3.6\, R_P L^4/v \tag{12.9}$$

where R_P is the planetary radius and B_A is the magnetic field strength at the top of the atmosphere.

Wave amplitudes required for strong diffusion

The strong diffusion lifetime (12.9) places an absolute upper limit on the rate of removal of radiation belt particles; this is valid irrespective of the intensity of the scattering waves. To obtain an estimate of the minimum fluctuating wave intensity required for strong diffusion scattering, one must first evaluate the effective rate of pitch-angle scattering for any particular resonant wave mode. In general, this involves a complex integration over wave frequency and $\bar{k}$-space together with a summation over each harmonic resonance [e.g., Lyons, Thorne, and Kennel, 1971]. For the case of electromagnetic waves this can be approximated by

$$\mathscr{D}_\alpha \approx \frac{\omega_c}{\gamma} \left(\frac{B'}{B} \right)^2 \tag{12.10}$$

where B′ is the total wide-band amplitude of the resonant fluctuating magnetic field [Kennel and Petschek, 1966]. For electrostatic waves polarized with $k_\perp/k_\parallel >> 1$, the effective pitch-angle scattering coefficient is

$$\mathscr{D}_\alpha \approx \frac{\omega_c}{\gamma} \left(\frac{\mathscr{E}'}{\beta B} \right)^2 \tag{12.11}$$

where $\beta = v/c$ and $\mathscr{E}'$ is the wide-band fluctuating electric field amplitude. In either case, the required minimum wave amplitudes can then be obtained by equating the bounce averaged diffusion coefficient to τ_{SD}^{-1}. This yields

$$B'_{SD} \approx (\gamma^2 - 1)^{1/4} (cB^2/3.6\ \delta\ R_P L^4 \omega_c)^{1/2} \tag{12.12}$$

and

$$\mathscr{E}'_{SD} \approx \beta\, B'_{SD} \tag{12.13}$$

where δ represents the fraction of the particle bounce orbit spent in resonance with the waves. For a dipole field with $\delta \approx 0.2$, one obtains numerical values

$$B'_{SD,e} \approx 10^2 (\gamma_e^2 - 1)^{1/4} L^{-7/2} nT \tag{12.14}$$

for relativistic electrons and

$$B'_{SD,p} \approx 3 \times 10^2 E_p^{1/4} (\text{keV})\, L^{-7/2} nT \tag{12.15}$$

for nonrelativistic protons with kinetic energy E_p. The corresponding strong diffusion electrostatic wave amplitudes are

$$\mathscr{E}'_{SD,e} \approx 3 \times 10^4 (\gamma_e^2 - 1)^{3/4} \gamma_e^{-1} L^{-7/2}\ \text{mV/m} \tag{12.16}$$

for relativistic electrons and

$$\mathscr{E}_{SD,p} \approx 10^2 E_p^{3/4} (\text{keV})\, L^{-7/2}\ \text{mV/m} \tag{12.17}$$

for nonrelativistic protons.

A comparison of the wave amplitudes required to scatter electrons and protons on strong diffusion at $L = 6$ is shown in Figure 12.1. Fortuitously, because the ratio between the surface magnetic field strength and the planetary radius is essentially the same for the Earth and Jupiter, this graph applies equally well to either magnetosphere. It is immediately clear that electrostatic waves have a lower threshold for causing strong diffusion scattering particularly in the case of nonrelativistic ions. For all nonrelativistic particles $B'_{SD} \sim m^{1/4} E^{1/4}$ whereas $\mathscr{E}'_{SD} \sim m^{-1/4} E^{1/4}$. For heavy ion scattering, the values plotted in Figure 12.1 would have to be scaled up or down by the fourth root of the ion atomic mass. As the particle energy increases, the conditions for strong diffusion scattering become more severe and the required power spectral density in electrostatic waves approaches that for electromagnetic waves. In either case, the required amplitudes scale as $L^{-7/2}$ so that strong-diffusion scattering is more likely to occur at large radial distance from the planet.

Possible waves for scattering and resonant particle energies

Within the terrestrial magnetosphere, four distinct classes of plasma waves have been identified that are capable of cyclotron resonant interaction with trapped radiation belt particles. These are the electromagnetic electron cyclotron (sometimes referred to as

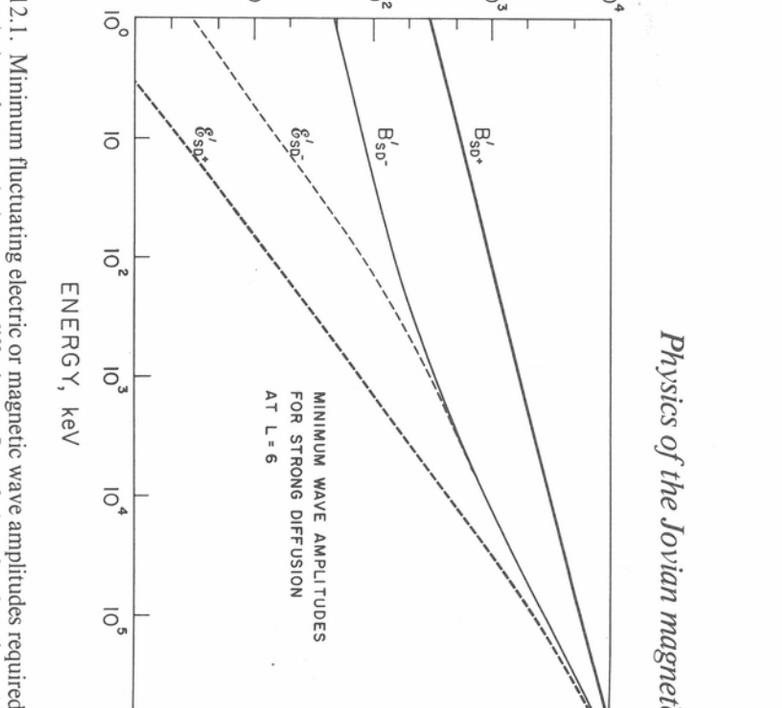

Fig. 12.1. Minimum fluctuating electric or magnetic wave amplitudes required to scatter protons (+) or electrons (−) or strong diffusion at $L = 6$. At other locations the required amplitudes scale as $L^{-7/2}$. The curves apply equally well to Earth or Jupiter.

whistler-mode) and ion-cyclotron waves, which are restricted to frequencies below the respective cyclotron frequency, and the electrostatic ion and electron cyclotron waves which typically occur in bands centered near odd half harmonics of the appropriate cyclotron frequencies ($n + 1/2)\omega_c$. For each class of wave, the observed spectral properties and typical resonant electron and ion energies [obtained from (12.3)] are presented in Table 12.1. Resonant energies with electromagnetic waves are controlled by the magnetic energy per particle $E_M = B^2/8\pi n$, while those for electrostatic waves are controlled by the thermal energy E_{th} of the plasma. The assumption has been made here that resonant ions are nonrelativistic, $E_{p,res} << E_{\omega,p} = m_p c^2$. Resonant electrons, however, must in general be treated as relativistic with $E_{e,res} \rightarrow E_{\omega,e}$ ($\gamma_{e,res}{}^2 - 1)/2$ in the nonrelativistic limit as $\gamma_{e,res} \rightarrow 1$.

Electromagnetic ion cyclotron waves are generally observed in the dusk sector or dayside region of the Earth's magnetosphere [Bossen, McPherron, and Russell, 1976]. This is consistent with theoretical expectations which favor most rapid instability in regions of enhanced plasma density [e.g., Cornwall, Coroniti, and Thorne, 1970; Thorne, 1972; Cuperman, Gomberoff, and Stemlieb, 1975] where the resonant ion flux should maximize. In such preferred regions, E_M is typically 1–10 keV. Electrons resonant with such waves are therefore relativistic ($\gamma_r >> 1$), while the resonant ion energies span the thermal population of the magnetosphere ring current. Because the observed broadband wave amplitudes are several nanotesla, the resonant particles can be subject to strong diffusion scattering (Fig. 12.1) leading to intense precipitation of relativistic electrons [Thorne and Kennel, 1971; Thorne, 1974] and ring current ions [Cornwall, Coroniti, and Thorne, 1970, 1971; Thorne, 1972].

Electromagnetic whistler-mode waves on the other hand occur throughout the terrestrial magnetosphere. A broadband hiss emission predominates at low L within the high density plasmasphere. This emission is thought to be the principal source of

Table 12.1. *Wave–particle resonant interactions*

	Electromagnetic		Electrostatic	
Waves class	Ion cyclotron	Whistler-mode	Ion cyclotron	Electron cyclotron
Observed terrestrial forms	Pcl, IPDP micropulsations	Sferics or whistlers plasmaspheric hiss outer zone chorus auroral hiss	Broad-band electrostatic noise	$(n+1/2)\omega_{c,e}$ harmonic bands ω_{UH} upper hybrid waves
Spectral properties	$\left(\frac{k_\parallel c}{\omega}\right)^2 \approx \frac{\omega_p{}^2}{\omega_{c,e}\omega_{c,p}} \frac{1}{(1-\omega/\omega_{c,p})}$	$\left(\frac{k_\parallel c}{\omega}\right)^2 \approx \frac{\omega_p{}^2}{\omega\,\omega_{c,e}} \frac{1}{(1-\omega/\omega_{c,e})}$	$k_\parallel \sim \frac{\omega_{c,p}}{v_{th,p}}$; $\omega \approx \left(n+\frac{1}{2}\right)\omega_{c,p}$	$k_\parallel \sim \frac{\omega_{c,e}}{v_{th,e}}$; $\omega \approx \left(n+\frac{1}{2}\right)\omega_{c,e}$
Resonant energies				
$(\gamma_{res,e}{}^2 - 1)\,E_{o,e}/2$	$E_M \left(\frac{m_p}{m_e}\right) \left(\frac{\omega_{c,p}}{\omega}\right)^2 \left(1 - \frac{\omega}{\omega_{c,p}}\right)$	$E_M \left(\frac{\omega_{c,e}}{\omega}\right) (1 - \omega/\omega_{c,e})^3$	$E_{th,p} \left(\frac{m_p}{m_e}\right) \left(\frac{\ell}{k_\parallel \rho_p}\right)^2$	$E_{th,e} \left(\frac{n - \ell + \frac{1}{2}}{k_\parallel \rho_e}\right)^2$
$E_{res,p} = \frac{m_p v_{res,p}{}^2}{2}$	$E_M \left(\frac{\omega_{c,p}}{\omega}\right)^2 \left(1 - \frac{\omega}{\omega_{c,p}}\right)^3$	$E_M \left(\frac{m_p}{m_e}\right) \left(\frac{\omega}{\omega_{c,e}}\right) \left(1 - \frac{\omega}{\omega_{c,e}}\right)$	$E_{th,p} \left(\frac{n - \ell + \frac{1}{2}}{k_\parallel \rho_p}\right)^2$	$\left(\frac{m_p}{m_e}\right) E_{th,e} \left(\frac{n + \frac{1}{2}}{k_\parallel \rho_e}\right)^2$

weak-diffusion scattering [Lyons, Thorne, and Kennel, 1972] for energetic electrons ($\gtrsim$ 50 keV) leading to the formation of the slot between the inner and outer radiation belts [Lyons and Thorne, 1973]. Intense bursts of "chorus" emissions occur in the outer zone during substorm periods [Tsurutani and Smith, 1974, 1977]. Observed wave amplitudes are sufficient to drive resonant electrons onto strong diffusion, leading to intense precipitation into the atmosphere. For either emission, the resonant ions are typically in the energy range above an MeV and the rate of pitch-angle scattering is relatively weak.

Both classes of observed electrostatic waves are polarized with $k_\perp >> k_\parallel$. For such oblique waves, higher-order cyclotron resonances become important, thus broadening the resonant energy range. This is in sharp contrast to the case of nearly parallel propagating electromagnetic waves where first order resonance predominates. Terrestrial electron electrostatic waves occur predominantly near the equatorial plane [Kennel et al., 1970; Christiansen et al., 1978; Kurth et al., 1979b] in the outer radiation zone. They are considered to be important in scattering plasma sheet electrons leading to diffuse auroral precipitation [Lyons, 1974]. Analogous waves at frequencies just above the proton cyclotron frequency are characteristically present on auroral field lines [Gurnett and Frank, 1977]. Precise frequency resolution into the anticipated harmonic band structure is not possible using satellite-borne instruments because of the large Doppler shift caused by the satellite motion. The observed waves therefore appear as broadband electrostatic noise, but the measured amplitudes appear to be sufficient to account for the observed diffuse auroral ion precipitation [Ashour-Abdalla and Thorne, 1977, 1978].

12.3. Plasma instability and quasilinear scattering in the Jovian magnetosphere

The spectral properties of plasma waves observed in the Jovian magnetosphere (Chapter 8 of this volume), together with simultaneous information on the trapped particle population (Chapters 4 and 5) can be utilized to both identify the potential mechanisms for wave instability and evaluate the rate of scattering loss of the resonant particles. The linear growth or damping rate of any particular wave mode can be expressed in terms of velocity-space gradients in the resonant particle distribution function [e.g., Kennel and Wong, 1967; Melrose, 1968]. The interested reader is referred to Chapter 9 (Sec. 9.2) for a summary of the basic formalism. Because the Landau ($\ell = 0$) resonant growth rate is directly proportional to $\partial f_o/\partial v_\parallel$, it will in general lead to wave attenuation. Landau amplification, however, can occur if the plasma carries a net current (i.e., an electron drift relative to the ions) or if there is a high-energy particle beam moving relative to the thermal population. Cyclotron ($\ell \neq 0$) resonant growth, on the other hand, can occur when the plasma exhibits a pitch-angle anisotropy (e.g., due to the mirror magnetic field geometry) or positive gradients in perpendicular velocity space $\partial f_o/\partial v_\perp > 0$. In our subsequent discussion, the observed distribution of various plasma waves is compared with theoretical expectations, and the wave intensities are employed to compute the rate of velocity space scattering.

However, before analyzing the specifics of any particular wave-particle resonance, it is useful to review certain general properties of energetic particle injection and removal from the Jovian radiation belts. In the absence of a local acceleration source, a steady-state solution to the radial diffusion equation (12.2) requires a balance between the cross-L transport and precipitation loss:

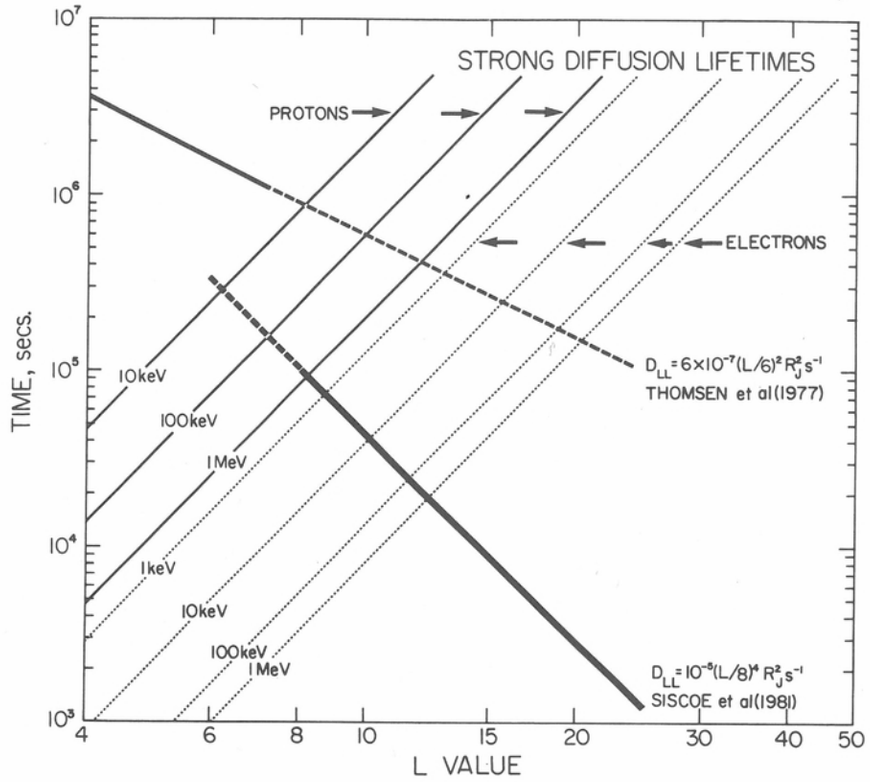

Fig. 12.2. Strong-diffusion lifetimes for energetic electrons and protons as a function of radial location in the Jovian magnetosphere. Two estimates of the time-scale for radial diffusion, $\tau_D \sim D_{LL}^{-1}$, are shown for comparison. The results are strictly valid only over the solid regions of the curves. The empirically determined results of Thomsen et al. [1977] represent an upper limit for diffusion driven by ionospheric winds. The results of Siscoe et al. [1981] are deduced from the distribution of heavy ions in the Io torus and have been interpreted in terms of centrifugally driven interchange instability.

$$L^2 \frac{\partial}{\partial L}\left[\frac{D_{LL}}{L^2}\frac{\partial f_o}{\partial L}\right] = \frac{f_o}{\tau_L} \tag{12.18}$$

Representative (empirically determined) values for the time-scale of radial diffusion $\tau_D \sim D_{LL}^{-1}$ caused either by centrifugual driven interchange instability of heavy ions in the outer region of the Io plasma torus [Froidevaux, 1980; Siscoe and Summers, 1981; Siscoe et al., 1981] or by neutral winds in the Jovian ionosphere [e.g., Brice and McDonough, 1973; Thomsen et al., 1977] are illustrated in Figure 12.2. [One should note that, in contrast to Jupiter, both interchange instability and neutral atmospheric winds provide relatively ineffective radial diffusion in the terrestrial magnetosphere.] Also shown for comparison are the minimum lifetimes (12.9) of electrons and protons subject to strong diffusion pitch-angle scattering. In the outer magnetosphere, where the rate of radial diffusion exceeds the rate of precipitation loss ($D_{LL}\,\tau_L >> 1$), rapid cross-L transport leads to a uniform plasma distribution function ($f_o(L) \approx$ constant). For a given magnetic moment, $\mu = p_\perp^2/2mB$, the differential flux $j(E) = p^2 f$ thus scales in direct proportion to the ambient field strength

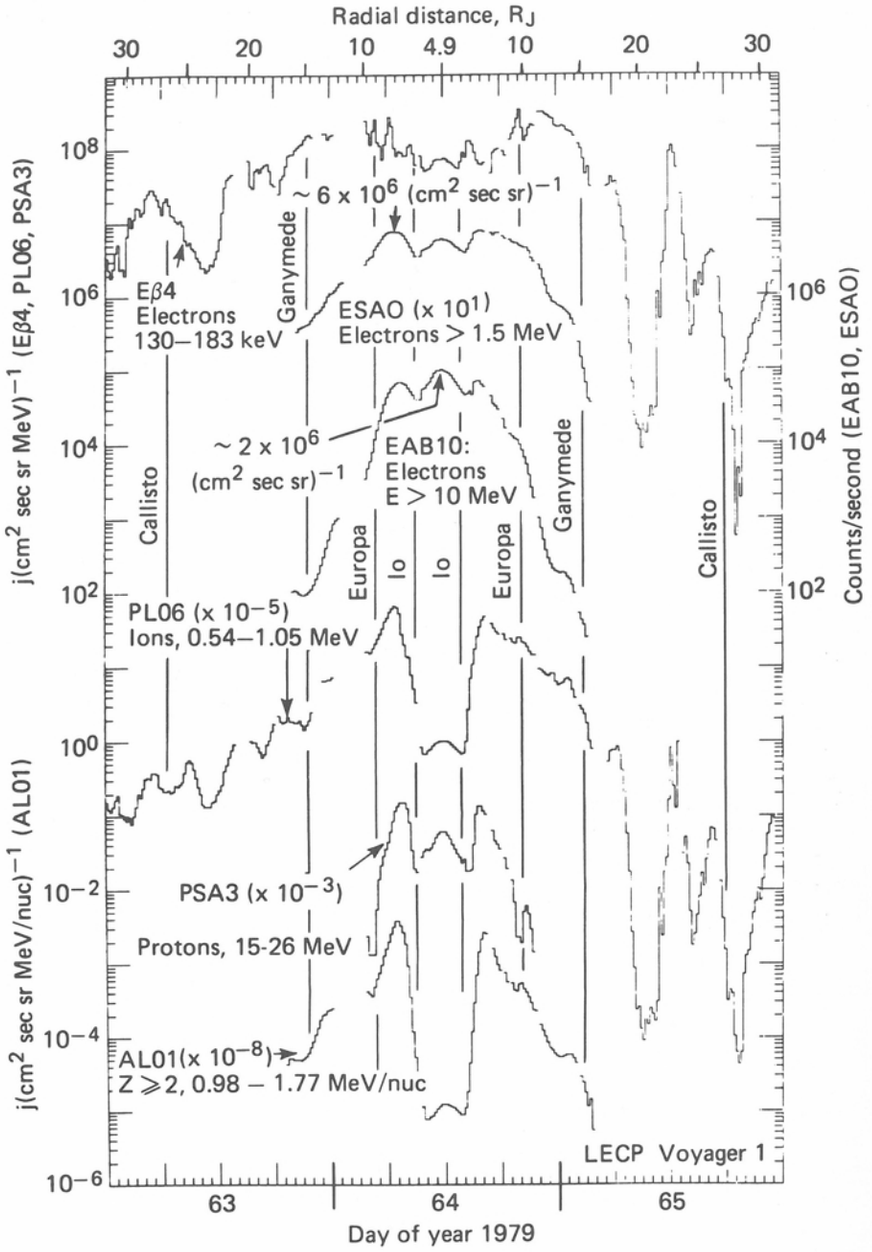

Fig. 12.3. Energetic charged particles measured in the inner Jovian magnetosphere by the LECP instrument on Voyager 1 [Krimigis et al., 1979a].

$j(\mu = \text{constant}) \sim L^{-3}$. The corresponding integral flux $J(> E)$ scales as $L^{-4.5}$ or L^{-6} depending on whether or not the particle energies are relativistic [e.g., Thorne and Coroniti, 1972]. However, once the rate of removal exceeds the rate of injection (namely at lower L), the particle distribution function develops a steep radial gradient to maintain a balance in (12.18) between injection and loss. As long as other transport processes (e.g., convection; Chapters 10 and 11) are relatively weak, one expects the energetic particle flux to peak near the region where $D_{LL}\,\tau_L \approx 1$.

The energetic particle fluxes observed on Voyager 1 [Krimigis et al., 1979a] exhibit clear examples of an inward diffusion induced precipitation boundary in the inner magnetosphere (Fig. 12.3). There is little evidence for pronounced longitudinal asymmetry that would be expected if large scale convection were the dominant transport mechanism. A comparison of the relevant time scales in Figure 12.2 suggests that ions with $E_p \sim 1$ MeV must be scattered near the strong diffusion rate to account for the pronounced flux depletion inside $L \approx 8$. The modest drop in energtic (> 1.5 MeV) electron flux in approximately the same location (upper panels of Fig. 12.3) requires only weak pitch-angle scattering. Mechanisms responsible for the ion and electron loss are discussed in more detail below. We simply note here that the combined ion and electron observations support the concept that inward diffusion driven in response to interchange instability of heavy torus ions provides the dominant source for energetic particles in the middle Jovian magnetosphere exterior to the orbit of Io. This conclusion does not rule out the possible importance of large scale convection as a viable transport mechanism for the thermal plasma [e.g., Hill, Dessler, and Maher, 1981] but, in contrast to the Earth's magnetosphere, convection does not appear to be a major source for the Jovian ring current plasma.

Inward diffusion also tends to enhance the pitch-angle anisotropy of the energetic particles (because the equatorial perpendicular and parallel momenta scale as $p_\perp \sim L^{-3/2}$ and $p_\parallel \sim L^{-1}$ for constant μ and J) and thus also provides a source of free energy capable of exciting plasma instabilities. Even when pitch-angle scattering becomes strong, inward diffusion can maintain a reasonable level of anisotropy in the region where $D_{LL}\,\tau_L >> 1$. The necessary conditions for instability of various plasma waves are discussed below, and a comparison is made with Voyager observations.

Whistler-mode waves

Figure 12.4 contains an overview of plasma waves observed on Voyager 1 near closest approach to Jupiter [Scarf et al., 1979a]. Several distinct classes of waves can be identified; we concentrate first on waves below the electron cyclotron frequency. As already discussed in Chapter 8 of this volume, definitive identification of the wave mode is impossible because the Voyager plasma wave instrument only measures fluctuating electric fields. Nevertheless, the spectral characteristics of the waves observed well above the proton gyrofrequency but below the electron cyclotron frequency suggest that the dominant emissions are analogous to terrestrial electromagnetic whistler-mode hiss and chorus. Auroral hiss [Gurnett, Kurth, and Scarf, 1979b] and discrete lightning generated whistlers [Gurnett et al., 1979b] are not considered here because their amplitudes are relatively weak (see Chapter 8), and the waves consequently have little effect on the trapped particles.

Although the spectrum channel data provide a useful overview of the wave spectral properties, the distinction between chorus and hiss is more apparent in the wide-band analog data. Examples of these high-resolution data have been shown in Figures 14 and 15 of Chapter 8. The most persistent and intense wave emission in the inner Jovian magnetosphere is a band of hiss with a peak power spectral intensity near a few hundred hertz, namely below the lower-hybrid resonance frequency. As illustrated in Figure 12.4 the intensity of this broadband emission is dramatically enhanced within the high-density torus surrounding the orbit of Io. Chorus-like emissions, on the other hand, occur intermittently. The wave frequency is typically centered near $\omega_{c,e}/2$ and the waves are confined to the magnetic equatorial region.

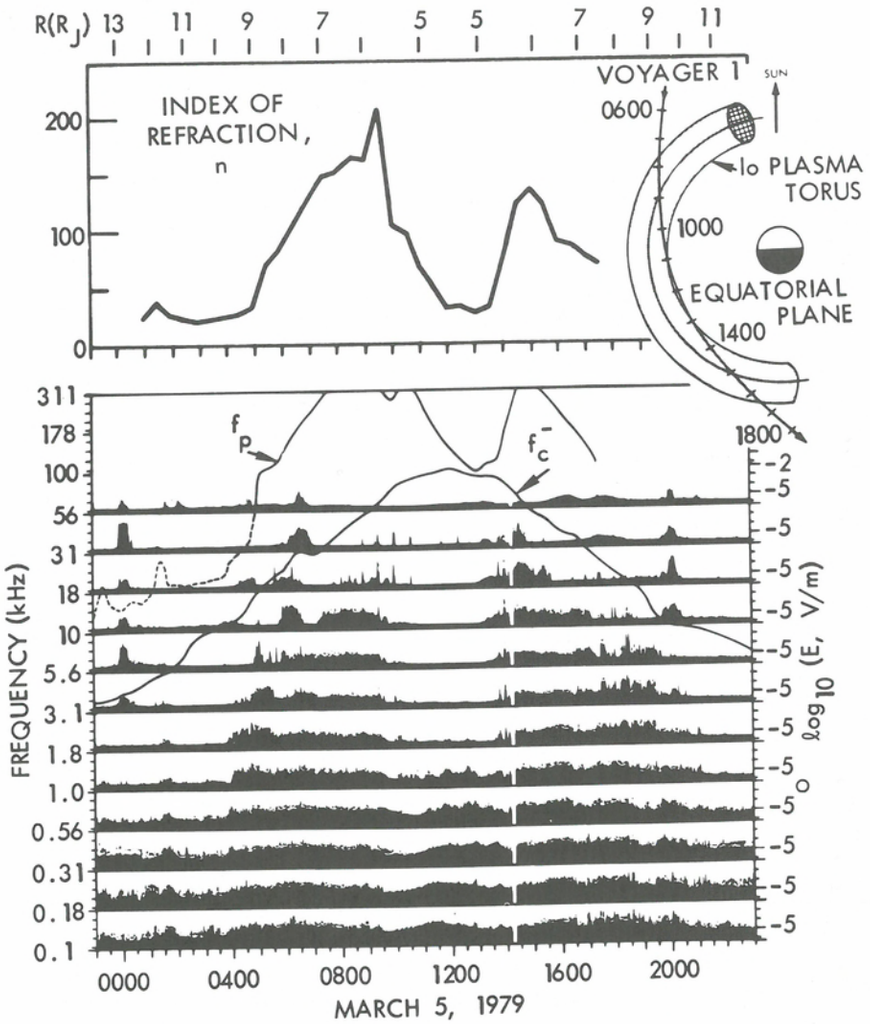

Fig. 12.4. Voyager 1 plasma wave observations near closest approach [Scarf et al., 1979a]. Preliminary values for the plasma frequency and electron gyrofrequency are shown for comparison. The index of refraction (top panel) can be employed to infer the fluctuating magnetic field intensity, which is dominant for whistler-mode signals.

A potential candidate for the generation of either electromagnetic emission is cyclotron resonant instability, driven by pitch-angle anisotropy in the electron distribution. For relativistic electrons, computation of the wave growth (or damping) rate involves a complicated integration along the resonance contour (12.3) which is hyperbolic in momentum space [Liehmohn, 1967; Schulz and Vampola, 1975; Barbosa and Coroniti, 1976]. A much simpler and more physically understandable result is obtained in the nonrelativistic limit [e.g., Kennel and Petschek, 1966]; the temporal growth rate for parallel propagating whistler-mode waves can then be expressed analytically as

$$\gamma_{cyc} \approx \pi\omega_{c,e}\left(1 - \frac{\omega}{\omega_{c,e}}\right)^2 \eta_e(v_{res})\,(A_e(v_{res}) - A_c) \tag{12.19}$$

where

$$\eta_e(v_{res}) = 2\pi\, v_{res} \int_0^\infty v_\perp f_{o,e}(v_\perp, v_\parallel = v_{res})\, dv_\perp \tag{12.20}$$

is the fractional number of resonant electrons,

$$A_e(v_{res}) = \left.\frac{\int_0^\infty v_\perp \tan\alpha\, \dfrac{\partial f_{o,e}}{\partial\alpha}\, dv_\perp}{2\int_0^\infty v_\perp f_{o,e}\, dv_\perp}\right|_{v_\parallel = v_{res}} \tag{12.21}$$

is the pitch-angle anisotropy of resonant electrons and

$$A_c = \left(\frac{\omega_{c,e}}{\omega} - 1\right)^{-1} \tag{12.22}$$

is the critical anisotropy, required for instability. This nonrelativistic cool plasma approximation (12.19) will generally be adequate for our discussion of instability in the high density region of the Io plasma torus.

Because the resonant electron energy (Table 12.1) is proportional to $B^2/8\pi n$, the high density plasma torus is a region of lower resonant energy and (for an electron energy spectrum decreasing with E) correspondingly higher resonant flux. Characteristic values for $B^2/8\pi n$ are sketched in Figure 12.5; they range from a few keV inside the equatorial torus to several hundred keV at higher latitudes (or low $L < 5$). This variation effectively confines instability to a limited region near the equatorial plane. The net gain G in wave power during field aligned transit across the unstable equatorial region (of length ℓ^*) is given by $\ln G = 2\gamma_{cyc}\ell^*/v_g$, where v_g is the average wave group speed. To ensure significant wave amplification, the resonant integral electron flux must exceed a critical value

$$J_e^*(E_e > E_{res}) \approx \frac{B}{A_e - A_c} \cdot \frac{\ln G}{\ell^*} \cdot \frac{c}{2\pi^2 e} \tag{12.23}$$

which is equivalent to the maximum stably trapped flux defined earlier by Kennel and Petschek [1966]. For $\ln G \approx 3$ ($\approx$ 20 fold increase in wave power), $\ell^* \sim 2R_J$ and $A_e - A_c \sim 0.2$ the critical flux for wave instability in the Io plasma torus is approximately

$$J_e^* \approx 10^{14}\, L^{-3}/\mathrm{m}^2\,\mathrm{s} \tag{12.24}$$

The variation in J_e^* with L is slightly different from the dependence in the terrestrial magnetosphere [Kennel and Petschek, 1966] owing to the assumption here that instability in the torus is restricted to the limited equatorial region controlled by centrifugal confinement of ions injected from Io. A more precise relativistic treatment of the wave growth [Barbosa and Coroniti, 1976] yields a result almost identical to (12.24) and this value will therefore be used in our subsequent discussion.

From (12.19) and (12.22), it is clear that cyclotron damping provides a natural upper limit to the band of unstable waves at a normalized frequency

$$(\omega/\omega_{c,e})_{\max} \approx A_e/(1 + A_e) \tag{12.25}$$

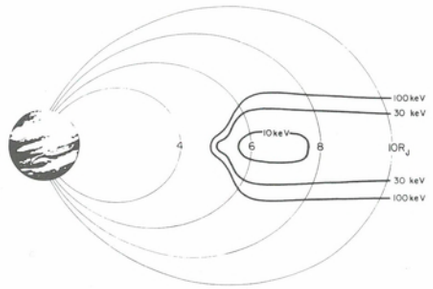

Fig. 12.5. The scaling energy $B^2/8\pi n$ for electromagnetic wave-particle resonance as a function of location in the vicinity of the Io plasma torus. This energy exceeds an MeV at high latitude and attains minimum values below 10 keV in the high density equatorial torus.

Furthermore, because the resonant electron energy (Table 12.1) increases as $\omega/\omega_{c,e}$ decreases, one can expect fewer resonant electrons and correspondingly weaker amplification at low frequency. From the resonant electron energies given in Table 12.1, one can therefore estimate a lower frequency limit to the unstable wave spectrum,

$$(\omega/\omega_{c,e})_{\min} \approx \frac{(\omega_{c,e}/\omega_p)^2}{(\gamma_{res,e}^{\ 2} - 1)_{\max}} \tag{12.26a}$$

or in the nonrelativistic limit

$$(\omega/\omega_{c,e})_{\min} \approx E_M/E_{e,\max} \tag{12.26b}$$

where $E_{e,\max}$ is the maximum resonant electron energy for which $J(E_e > E_{e,\max}) \gtrsim J_e^*$.

A comparison between the critical flux required for instability (12.24) and electron fluxes observed at three locations on Voyager 1 is shown in Figure 12.6. The plotted integral flux has been computed from direct measurements of the integral spectrum above 1.5 and 10 MeV reported by Krimigis et al. [1979a], differential fluxes in the energy range 130–183 keV [Krimigis et al., 1979a] and values of the low energy ($E \lesssim 4$ keV) electron distribution function $f_{o,e}(v)$ [Scudder et al., 1981], which can be employed to obtain the differential flux $j_e(v) \sim v^2 f_{o,e}(v)/\gamma m_e$. At $L = 18$, the entire electron population below ≈ 1 MeV lies above the critical flux required to excite whistler-mode emissions. Intense instability can therefore be anticipated over a broad range of frequency. In the absence of a strong particle source, one would expect pitch-angle scattering to eventually reduce the flux to the critical level J_e^* [Kennel and Petschek, 1966]. However, at $L \approx 18$, interchange driven radial diffusion is considerably more rapid than precipitation loss, even under strong pitch-angle diffusion (see Fig. 12.2). The observed electron flux profile should therefore be controlled by inward radial transport from the outer Jovian magnetosphere. However, we have already established that the integral electron flux in the diffusion dominated regime should scale as $J(>E) \sim L^{-4.5}$ or L^{-6} depending on whether or not the electrons are relativistic. The relative increase in the inward diffusing flux is therefore larger than the increase in $J_e^*(L)$, and values exceeding J_e^* consequently occur in the inner magnetosphere. This concept of a radial diffusion dominated region in the outer Jovian magnetosphere was discussed earlier by Thorne and Coroniti [1972], Coroniti [1974] and Coroniti et al., [1974]. The only difference here is our use of the more rapid rate of radial transport by interchange instability [Siscoe and Summers, 1981] rather than ionospheric winds or solar-wind induced electric fields.

At $L \approx 7.7$, the integral flux of electrons at energies below ~ 600 keV is also above the critical level; instability can again be anticipated over a broad range of frequency. However, the extent by which J_e exceeds J_e^* is less dramatic and a comparison between the observed fluxes at 7.7 and those anticipated on the basis of adiabatic transport from $L = 18$ (the dashed line) indicates a significant departure from simple loss-free inward

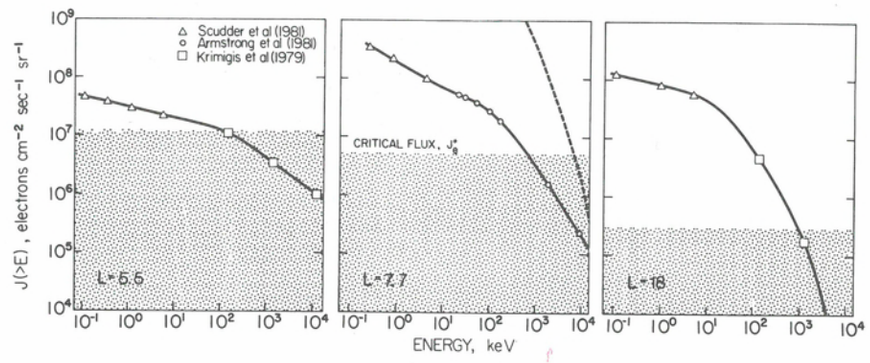

Fig. 12.6. The integral electron flux observed on Voyager at three locations in the middle Jovian magnetosphere is compared to the anticipated critical flux for onset of electron-cyclotron resonant instability with electromagnetic whistler-mode waves. For $L \gtrsim 7.7$, intense instability is predicted over a broad range of resonant frequency. The observed flux at $L = 7.7$ is consequently smaller than the value predicted (dashed line) on the basis of loss-free inward diffusion from $L = 18$. In the region of relatively slow inward diffusion inside the orbit of Io, rapid scattering loss has depleted the flux at $L = 5.5$ to values comparable to the stably trapped level.

injection. But because the timescale for strong diffusion loss is much smaller than the radial diffusion time at $L \approx 7.7$ (Fig. 12.2), it is clear that energetic electrons in the torus are subject only to weak diffusion scattering. In fact, to reach this location the electron precipitation lifetimes must typically exceed $\sim 10^5$ s. From (12.10) an upper limit can be placed on the allowed power spectral intensity of the resonant whistler-mode waves, which, as shown later, is generally consistent with the average properties of observed waves in this region of the torus.

Compelling evidence for the reduction in trapped electron flux to the critical stably trapped level J_e^* is apparent at $L = 5.5$. The entire electron population between 1 and 100 keV lies within a factor of three of the predicted level. This reduction is also consistent with the marked decrease in the observed wave intensities inside this location (Fig. 12.4). Radial diffusion inside the orbit of Io is apparently no longer able to provide an effective source to combat even weak diffusion losses in the inner torus. A dramatic change in the dominant mechanism for radial transport is anticipated inside $L \approx 5.9$ [Richardson et al., 1980] because centrifugually driven interchange instability can only carry Io injected ions to larger L. Radial diffusion inside the orbit of Io is probably driven by neutral winds in the Jovian ionosphere but even the most optimistic estimates for such transport (see Fig. 12.2) yields cross-L diffusion times in excess of 10^6 seconds.

The integral electron fluxes observed on Voyager [Krimigis et al., 1979a] have been employed by Thorne and Tsurutani [1979] to predict the lower frequency cut-off (12.26) of unstable whistler-mode waves in the vicinity of the Io plasma torus. Their results are reproduced here in Figure 12.7. The rapid increase in f_{min} inside $L \approx 5.5$ is mainly caused by the dramatic increase in the electromagnetic resonant scaling energy $B^2/8\pi n$ owing to lower plasma density inside the orbit of Io. The observed waves (Fig. 12.4) generally lie within the theoretically predicted unstable band. The only notable discrepancy is the existence of very low frequency ($\lesssim 1$ kHz) waves inside $L \sim 5.5$. This feature, however, can be understood [Scarf et al., 1979] in terms of waves originating within the torus and subsequently propagating to lower L across the

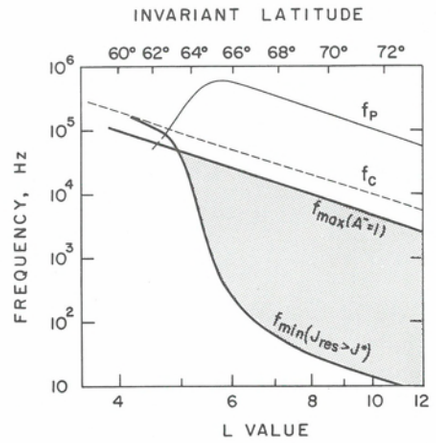

Fig. 12.7. The predicted band (shaded) of unstable cyclotron resonant whistler-mode waves in the inner Jovian magnetosphere compared to the equatorial cyclotron $f_{c.e}$ and plasma frequency f_p. The upper frequency cut-off is controlled by the available pitch-angle anisotropy (here assumed to be $A_e \approx 1$) of resonant ($\approx$ 1 keV) electrons. The lower frequency cut-off is determined by the maximum energy of electrons with flux J_{res} exceeding the threshold for significant wave growth. The steep increase in f_{min} inside $L = 6$ is mainly due to the dramatic increase in resonant electron energy at low L. The predicted unstable band is generally consistent with Voyager observations [Scarf et al., 1979a].

magnetic field lines, which is possible only at frequencies below the lower hybrid resonance frequency.

Although the general properties of the observed whistler-mode waves are consistent with a cyclotron-resonant instability, the detailed spectral properties have yet to be understood. The occurrence of chorus at frequencies above $f_{c.e}/2$ requires the presence of resonant $\sim$ keV electrons with substantial pitch-angle anisotropy, $A_e > 1$ (see 12.25). Furthermore, the intermittent bursty nature of chorus suggests rapid temporal variations in either the flux or the anisotropy of low-energy resonant electrons. But it has already been shown in Figure 12.6 that the flux of $\sim$ keV electrons at $L \approx 7.7$ and 18 is approximately two orders of magnitude above the level required for instability. The intermittent nature of chorus must therefore be related to variability in the electron anisotropy. The absence of intense chorus emissions over most of the Voyager trajectory through the torus can realistically be explained only by requiring that the pitch-angle anisotropy be small ($A_e << 1$) for the low-energy electron population. This could be maintained by processes such as Coulomb collisions or by pitch-angle scattering by other plasma waves. As an example, the characteristic time for Coulomb isotropization (i.e., the time to scatter one radian) of electrons is $\tau_c \sim 3 \times 10^8 E_e^{3/2}$ (keV)/n seconds. Coulomb scattering should therefore be effective at maintaining an isotropic low energy ($E_e < 1$ keV) distribution in the high density ($n \sim 10^3$ cm^{-3}) torus where τ_c is less than the timescale for inward radial diffusion. Unless some additional rapid source for injecting $\approx$ keV electrons with flat pitch-angles ($\alpha \sim \pi/2$) is available, high-frequency ($\omega/\omega_{c.e} \gtrsim 1/2$) whistler-mode waves could not be excited in the high density torus, and this is consistent with the absence of chorus at low L. However, in the outer torus ($L \gtrsim 8$) where $N \lesssim 10^2$ cm^{-3}, the characteristic Coulomb deflection time for $E_e \sim 1$ keV exceeds the interchange radial diffusion time (Fig. 12.2) and, inward diffusion could therefore establish significant electron anisotropy. Stochastic acceleration by intense electrostatic waves provides an alternative source for anisotropic low energy electrons (see the following section). The confinement of such waves to the equator might also explain why the observed chorus emissions are located near the equatorial plane since the perpendicular adiabatic acceleration is most effective there.

When chorus is observed the emission is particularly intense. The example reported by Coroniti et al., [1980] (also see Fig. 8.15), which occurred near $L \sim 8$ at 0620:45, had a wide band amplitude of approximately 10 picotesla. By scaling the

required strong diffusion amplitudes given in Figure 12.1 to $L \approx 8$, it is clear that such waves are sufficient to drive resonant ($\approx$ keV) electrons into strong pitch-angle diffusion. The concomitant rapid pitch-angle scattering should lead to a relaxation of the anisotropy and thus provides a natural explanation for the bursty nature of the emission.

Why broadband hiss should be most intense at frequencies well below the electron cyclotron frequency is also something of a puzzle. The peak growth rate (12.19) should typically occur at frequencies just below the upper cut-off (12.25); unless the electron anisotropy is exceedingly small, one would normally expect the most intense waves near a few tenths of the electron cyclotron frequency. This is clearly not the case, which suggests that propagation effects might play an important role in the origin of Jovian hiss as it does for similar waves in the Earth's plasmasphere [Thorne et al., 1980], but this conjecture also remains to be tested.

On the assumption that the emissions observed below the electron cyclotron frequency are indeed propagating in the whistler-mode, one can use the measured fluctuating electric fields to obtain estimates for the rate of resonant particle pitch-angle scattering. If the waves are polarized with $\bar{k}$ parallel to $\bar{B}$, the fluctuating magnetic field, $B'(f) = n_{\|}\, \mathscr{E}'(f)$. This is also a reasonably good approximation for oblique propagation. Because the whistler-mode refractive index is high ($n_{\|} \approx$ 10–100) within the torus (see Fig. 12.4), the fluctuating power spectral density is dominated by the wave magnetic field. One can therefore use (12.10) to evaluate the resonant pitch-angle diffusion coefficient. Independent estimates for the rate of scattering by the observed broadband hiss [Scarf et al., 1979a; Thorne and Tsurutani, 1979] indicate that the diffusion is most rapid for electrons above 100 keV. Figure 12.8 (from Scarf et al., [1979a]) provides a summary of the average scattering properties at different locations near the inner edge of the plasma torus. The top panels show the average fluctuating electric fields observed by Voyager 1 during four 96 s intervals. The lower panels display the computed wave refractive index, the fluctuating magnetic field, the resonant electron energy, and the anticipated timescale for local pitch-angle scattering ($\tau_s \sim 1/D_{\alpha\alpha}$) near the orbit of Voyager. Because the wave-particle interactions should be strongly confined to the equatorial torus region, electrons spend a small fraction ($\delta \sim 0.1$) of their orbit in resonance. The timescale for precipitation loss to the atmosphere is consequently an order of magnitude longer than the scattering times shown in Figure 12.8. Nevertheless, the expected rate of removal of relativistic electrons in resonance with $f \lesssim 1$ kHz waves can become very rapid. For example, at 1530 (near $L \approx 6$) the electron lifetime for $E_e \gtrsim 500$ keV is typically between 10^4 and 10^5 s. Although this is longer than the lifetime expected under strong pitch-angle diffusion it is considerably shorter than the most optimistic estimates for radial diffusion times in the vicinity of Io, as exhibited in Figure 12.2.

In the absence of a strong source capable of accelerating electrons locally to relativistic energies, the energetic ($\gtrsim$ MeV) electron flux would be rapidly depleted by such intense scattering. Furthermore, because the flux of relativistic electrons is generally below J_e^* (see Fig. 12.6) the pitch-angle diffusion is parasitic in the sense that the scattering waves are produced by lower energy electrons. Similar parasitic scattering occurs in the Earth's plasmasphere [Lyons et al., 1972] leading to an almost total removal of energetic electrons between the inner and outer radiation belts [Lyons and Thorne, 1973]. Because the removal of relativistic (> MeV) electrons is not expected to be limited by the stably trapped flux, rapid precipitation loss poses a serious question on whether inward radial diffusion can provide a viable source of synchrotron radiating electrons in the inner Jovian magnetosphere as discussed by Coroniti [1974]. It also appears unlikely that corotating convection [Hill, Dessler, and Maher, 1981] provides a more rapid transport mechanism because the anticipated longitudinal asymmetries

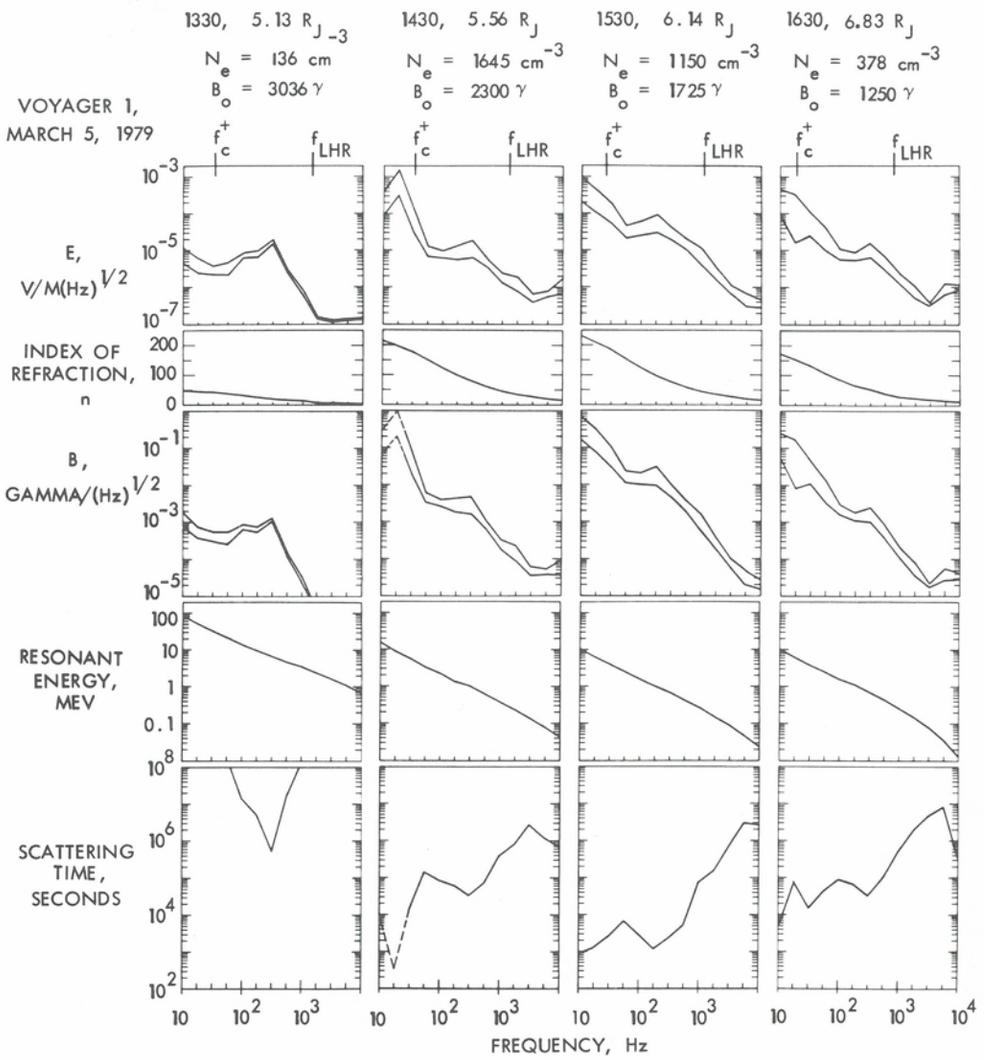

Fig. 12.8. Detailed analyses of the wave particle interactions for four 96 s intervals as Voyager 1 traveled from the inner edge of the plasma torus (1330) to the outer torus region (1630) [Scarf et al., 1979b]. The plasma density and magnetic field strength for the four intervals are: (1330) $n_e = 136$ cm^{-3}, $B_o = 3036$ gammas; (1430) $n_e = 1645$ cm^{-3}, $B_o = 2300$ gammas; (1530) $n_e = 1150$ cm^{-3}, $B_o = 1725$ gammas; (1630) $n_e = 378$ cm^{-3}, $B_o = 1250$ gammas. At the inner edge of the torus, the long local scattering times indicate that the electron distribution is relatively stable to precipitation losses. Within the torus, electrons with $E_e > 0.1$ MeV undergo strong local scattering and have precipitation lifetimes that may be comparable to radial diffusion source times.

have not been observed. There is, however, some uncertainty in the identification of the low frequency ($\lesssim$ 60 Hz) signals as exclusively whistler-mode waves [Scarf et al., 1979a]. The observed wave power spectral density is highly variable and often exhibits an enhancement associated with the proton gyrofrequency (see Fig. 12.8). One cannot exclude the possibility that electrostatic ion-mode waves contribute to the observed

low frequency emission. If so, the relativistic electron (< few MeV) scattering times would be much longer than the values exhibited in Figure 12.8.

Even at frequencies above 100 Hz, where the wave identification is more secure, the observed scattering wave amplitudes are highly variable (Fig. 12.8). Average precipitation lifetimes in the torus ($L \gtrsim 5.5$) probably exceed 10^5 seconds at energies near 1 MeV and rise to values above 10^6 s near 100 keV. Inward radial diffusion driven in response to interchange instability of the torus heavy ions should therefore provide an effective source of electrons, even at relativistic energies throughout most of the Io torus. Although the rate of inward diffusion should decrease dramatically inside the orbit of Io, the observed intensity of the scattering waves is also considerably lower. Furthermore, the scaling energy for resonance with electromagnetic waves, $B^2/8\pi n$, rise to values above 100 keV for $L \lesssim 5$ (Fig. 12.5), and even MeV electrons will have too low an energy to resonate with the residual low frequency ($\omega < \omega_{LH}$) waves which presumably originate in the torus (see panel 1 in Fig. 12.8). The relativistic ($\sim$ MeV) electrons observed at $L \approx 5.5$ (Fig. 12.6) should therefore experience relatively little depletion during their subsequent slow inward diffusion into the synchrotron radiating region ($L \lesssim 3$) of the inner Jovian magnetosphere. The initial Voyager 1 observations reported by Krimigis et al. [1979a], while limited to the region $L \gtrsim 4.9$, support these theoretical expectations. As shown in Figure 12.3, the energetic (> 1.5 MeV) electron flux exhibits significant depletion in the inner torus ($5.5 \lesssim L \lesssim 8$) but then increases with decreasing L in the inner magnetosphere ($L < 5.5$). In the absence of further scattering loss, the electron distribution function $f_o(\mu = \text{constant})$ should be conserved and by scaling the observed flux at $L = 5.5$ (Fig. 12.6) one can anticipate a relativistic ($E_e > 1$ MeV) integral spectrum $J_e(> E) \approx 2 \times 10^{12}/E_e$(MeV) electrons/m^2-s-sr at $L \approx 3$ near the outer portion of the synchrotron radiating region. It is also of interest to note that the lower energy portion ($E_e \approx$ MeV) of the synchrotron spectrum between ($2 \lesssim L \lesssim 3$) originates from electron fluxes ($E_e \approx$ keV) limited by whistler-mode stable trapping in the inner torus (Fig. 12.6); a concept initially suggested by Coroniti [1974]. However, the more energetic electrons ($E_e \gtrsim 10$ MeV) in the synchrotron region should be subject to parasitic scattering loss ($J_e << J^*$) during transit through the torus. Their flux could thus exhibit significant long-term variability, which should be reflected in the power of higher frequency decimetric radiation.

Electrostatic emissions above $\omega_{\vartheta,e}$

In addition to the broad-band whistler-mode emissions, Figure 12.3 shows several examples of waves above the electron cyclotron frequency that, in analogy with terrestrial observations, have been identified as electrostatic upper hybrid or electron cyclotron harmonic waves [Kurth et al., 1980b; also see Chapter 8, Sec. 8.4]. Both classes of wave occur in narrow frequency bands centered between multiples of the electron cyclotron frequency. Strong cyclotron damping by the thermal plasma is expected at exact multiples of $\omega_{c,e}$. Although highly variable, the wave intensities exhibit a systematic increase with decreasing radial distance and reach peak amplitudes of a few mV/m in the outer torus. The observed emissions are also very tightly confined (within a few degrees) to the magnetic equator; this limits the average rate of scattering of any resonant electrons.

Barbosa and Kurth [1980] have developed a theoretical model for the generation of the Jovian electrostatic waves using free plasma energy associated with a loss-cone distribution (for which $\partial f_o/\partial v_\perp > 0$) of suprathermal electrons superimposed on a dense thermal background plasma. This approach has been successfully used to explain

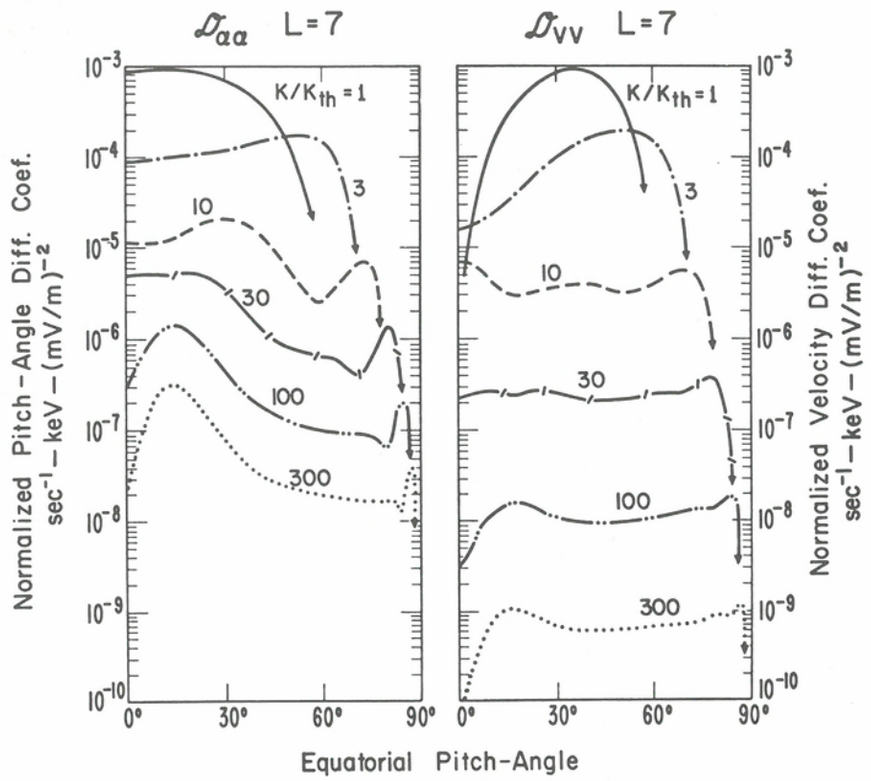

Fig. 12.9. Normalized coefficients for diffusion in pitch-angle ($D_{\alpha\alpha}$) and for diffusion in speed D_{vv}) plotted as a function of equatorial pitch-angle at $L = 7$ for representative values of the electron energy normalized to the thermal energy of the warm electrons [Lyons, 1974]. The actual bounce-orbit averaged diffusion coefficients can be obtained by multiplying $D_{\alpha\alpha}$ and D_{vv} by $|\mathscr{E}'|^2/K_{th}$ with $|\mathscr{E}'|$ expressed in mV/m and K_{th} expressed in keV.

electron harmonic waves in the terrestrial magnetosphere [Young, Cullen, and McCune, 1973; Ashour-Abdalla and Kennel, 1978a; Hubbard and Birmingham, 1978; Curtis and Wu, 1979]. Barbosa and Kurth [1980] have also computed wave ray paths to evaluate the net convective growth of unstable waves. Their theoretical simulation shows that waves originating only a few degrees away from the equator experience a rapid change in resonant velocity (12.3), which significantly reduces the total convective gain. Furthermore, waves amplified at the equator are effectively trapped (by their subsequent ray paths) leading to the observed equatorial confinement. Barbosa and Kurth [1980] have also made estimates for the critical electron flux required to produce significant convective wave amplification. Their "best" estimate requires an integral resonant electron flux J_e ($> E_{res}$) between 2×10^{11} and 6×10^{11}/m^2-s-sr to excite the first harmonic ($3f_{ce}/2$) band over the radial range $20 \lesssim L \lesssim 8$, respectively. Proportionately larger flux is required for higher $(n + 1/2)\, f_{ce}$ harmonic excitation. Even for the first harmonic band the required electron flux is considerably larger than J_e^* for whistler-mode instability (12.24), but a direct comparison with observed fluxes (see Fig. 12.6) indicates that anisotropic electrons in the energy range below $\approx$ 30 keV should nevertheless be able to excite the electrostatic waves in the outer torus. However, in the inner torus at $L \approx 5.5$, the marked reduction in trapped electron flux to the whistler

stably trapped level could quench the instability of electrostatic electron-cyclotron harmonic waves.

Provided that resonance is possible, the reported peak wave amplitudes (a few millivolts per meter) would appear to be marginally sufficient to cause strong diffusion scattering of low energy ($\lesssim$ 10 keV) electrons (see Fig. 12.1). However, because the observed waves are confined within a few degrees of the equator, resonant electrons spend only a few percent of their bounce orbit in the interaction region. Electric field amplitudes required for strong diffusion scattering consequently are about three times larger than shown in Figure 12.1. Even so, resonant $\approx$ keV electrons should still be strongly scattered by the most intense waves ($\mathscr{E}' \approx$ few mV/m) in the outer torus.

A detailed evaluation of the bounce averaged rate of pitch-angle scattering $D_{\alpha\alpha}$ and energy diffusion D_{vv} has previously been performed by Lyons [1974] for electrons resonant with narrow band first harmonic ($3\, f_{ce}/2$) waves in the Earth's magnetosphere. His generalized results, reproduced here in Figure 12.9, should apply equally well to Jupiter. It is clear that both energy diffusion and pitch-angle scattering are most effective for electrons near the thermal energy of the warm plasma. In the middle Jovian magnetosphere ($10 \lesssim L \lesssim 20$), characteristic electron thermal energies are probably near a few keV [Scudder et al., 1981]. The most rapid scattering by the narrow-band cyclotron harmonic waves should therefore occur for electrons below approximately 10 keV. At higher energies the relative rate of pitch-angle scattering scales as $D_{\alpha\alpha} \sim (E_e/E_{th})^{-3/2}$ and the energy diffusion rate $D_{vv} \sim (E_e/E_{th})^{-5/2}$.

Without detailed information on the electrostatic fluctuating electric field amplitudes as a function of L, only approximate estimates can be made for the resonant electron lifetimes. But we have already established that the peak wave amplitudes observed in the inner magnetosphere (a few mV/m) should be marginally adequate to scatter the thermal keV electrons on strong diffusion. To proceed, we assume that this is true throughout the middle magnetosphere; namely, the lifetime for $\sim$ keV electrons is given by the strong diffusion lifetime (12.9) plotted in Figure 12.2. However, as exhibited in Figure 12.9, the rate of scattering decreases with increasing electron energy. Energetic resonant electrons therefore are subject only to weak diffusion and the corresponding precipitation lifetime $\tau_L \approx \mathscr{D}_{\alpha\alpha}^{-1} \sim (E_e/E_{th})^{+3/2}$, which can be compared to the strong diffusion lifetime $\tau_{SD} \sim E_e^{-1/2}$. Provided that thermal electrons are never subject to pitch-angle diffusion at a rate exceeding the strong-diffusion level (which appears to be true for the keV electrons in resonance with electrostatic waves in the Jovian magnetosphere) the precipitation lifetime for energetic electrons can be simply expressed in terms of the appropriate strong diffusion lifetime (12.9) as

$$\tau_L(E_e)/\tau_{SD}(E_e) \approx (E_e/E_{th,e})^2\, [\tau_L(E_{th,e})/\tau_{SD}(E_{th,e})] \tag{12.27}$$

When the thermal ($\sim$ keV) electrons are indeed subject to strong diffusion, the energetic electron lifetime can be directly computed using Figure 12.2. For example at $L = 10$ the electrostatic scattering lifetime for 100 keV electrons would be (10^3 to 10^4)τ_{SD} or 10^7 to 10^8 s, which is much longer than the lifetimes established for scattering by whistler-mode hiss (see previous section). Because this estimate is based on the peak electrostatic wave amplitudes observed at Jupiter, it represents an absolute lower limit on the resonant electron lifetime. The nonadiabatic dynamics of energetic (> 100 keV) electrons is apparently controlled by whistler-mode waves throughout the middle magnetosphere.

Electrostatic waves were observed only when the Voyager trajectory lay within a few degrees of the magnetic equator, and even then the intensities were highly variable. It is therefore difficult to make precise estimates on their overall scattering properties. However, near $L \sim 8$ on the inbound trajectory, the plasma wave instrument

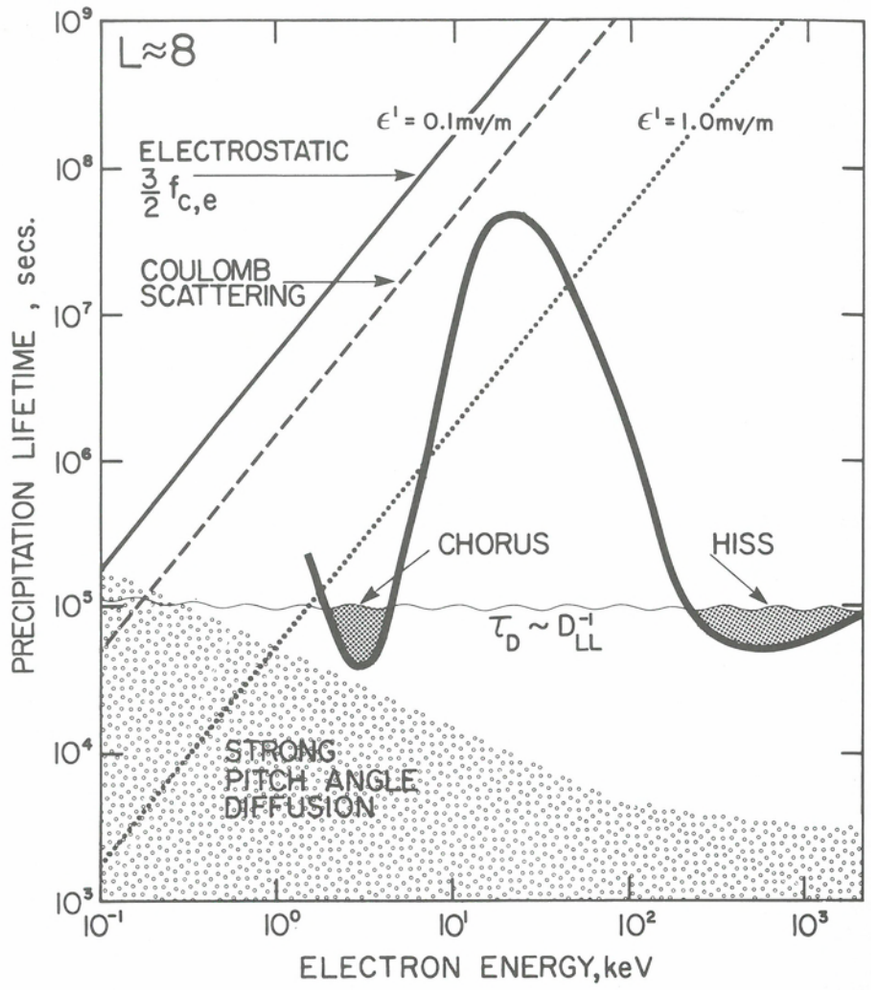

Fig. 12.10. Precipitation lifetimes for electrons resonant with electrostatic $3 f_{c,e}/2$ waves and electromagnetic whistler-mode chorus and hiss observed in the Io torus near $L \approx 8$.

detected electromagnetic hiss and chorus together with electrostatic cyclotron harmonic waves. It is therefore possible to compare scattering lifetimes directly in this region of the magnetosphere. The relevant electron pitch-angle scattering times due to resonance with the electromagnetic emissions have been evaluated by Thorne and Tsurutani [1979] and also shown in Fig. 8.15. The effective electron precipitation time has been plotted in Figure 12.10 by scaling these scattering times upward by a factor of 10 to account for the fraction of the electron orbit spent in resonance with the waves. As discussed in the previous section, the intense chorus emissions cause rapid removal of 3 keV electrons near the limit imposed by strong diffusion, while the scattering by hiss is most effective for electrons above 100 keV. At this location, both electromagnetic emissions appear to be able to remove resonant electrons at a rate comparable to interchange driven inward diffusion. The trapped electron flux consequently exhibits a marked depletion in phase space density at lower L; this is consistent with the high energy flux profiles reported by Krimigis et al. [1979a] (also see Fig. 12.3).

The maximum fluctuating electric field amplitude in the first $(3 f_{c,e}/2)$ harmonic band was approximately 10^{-1} mV/m near $L \approx 8$ (see Fig. 12.4); this should be compared to the amplitude $\mathscr{E}'_{SD,e} \approx 1$ mV/m required for strong diffusion scattering of thermal keV) electrons. The corresponding electron precipitation lifetimes are therefore approximately $\tau_L(E_{th}) \sim 100\ \tau_{SD}(E_{th})$ for thermal electrons and considerably longer (12.27) at higher energy. As illustrated in Figure 12.10, the expected precipitation lifetime due to resonance with the observed electrostatic waves exceeds the scattering time for electromagnetic resonant interactions over the entire energy range. The electrostatic scattering lifetimes are even longer than the angular deflection time due to Coulomb scattering in the torus assuming $n \sim 200$ [Bagenal and Sullivan, 1981]. It might therefore appear that the electrostatic waves are relatively unimportant at this location even for lower energy electrons. However, should the wave amplitudes reach values near 1 mV/m (which is entirely conceivable owing to the limited equatorial coverage on Voyager) the scattering by electrostatic waves would become significant at all energies below $\sim$ 50 keV. This could be particularly important for lower energy electron scattering in locations where chorus is not present.

A second potentially important role played by electrostatic plasma waves is their ability to provide stochastic acceleration. As exhibited in Figure 12.9, the rate of energy diffusion is comparable to that for pitch-angle diffusion for resonant electrons near the thermal energy, but it becomes progressively less important at higher energy. The net result of any energy diffusion is an acceleration of particles to higher energy in an attempt to flatten out the velocity space gradient. If the scattering waves are polarized with $k_\perp >> k_\parallel$ the acceleration occurs predominantly in the perpendicular direction. This tends to enhance the pitch-angle anisotropy of the thermal plasma and thereby provides an additional source of free energy to excite other plasma waves such as electromagnetic whistler-mode chorus (see previous section). For example, if the electrostatic $3 f_{c,e}/2$ waves near $L \approx 8$ attain amplitudes approaching 1 mV/m, localized energy diffusion could provide a source of thermal electrons ($E_e \lesssim$ few eV) at a rate comparable to or faster than cross-L transport (see Fig. 12.10). Furthermore, the predominantly perpendicular acceleration enhances the low-energy electron anisotropy at a rate significantly faster than that of Coulomb isotropization, thereby providing a viable mechanism for high frequency chorus excitation at this location. Because the timescale for energy diffusion is proportional to $(E_e/E_{th})^{5/2}$, perpendicular electrostatic acceleration becomes negligible above 10 keV. The band of unstable chorus excited by this acceleration should therefore be limited to frequencies comparable to or above $f_{c,e}/2$.

Possible waves for ion scattering

The radial profiles of energetic ions observed on Voyager 1 [Krimigis et al., 1979a; Armstrong et al., 1981; Lanzerotti et al., 1981] exhibit evidence for rapid precipitation loss in the inner ($L \lesssim 8$) torus (see Fig. 12.3). This depletion cannot be due to collisional processes such as Coulomb scattering or charge exchange because the relevant removal rates are much smaller than the anticipated rate of inward radial diffusion. Scattering by plasma turbulence offers the only viable loss mechanism and several possible scattering wave-modes have been considered.

Conditions for excitation of electromagnetic ion-cyclotron waves in the Jovian magnetosphere and their potential influence on trapped ions were initially discussed by Kennel [1972] and Thorne and Coroniti [1972] and more recently applied by Goertz [1980b] to describe the ion losses observed on Voyager. The instability is directly

analogous to the whistler-mode interaction with energetic electrons as outlined in an earlier section. The temporal growth rate for parallel propagating waves [e.g., Kennel and Petschek, 1966] is

$$\gamma_{cyc} \approx \frac{\pi}{2}\,\omega_{c,p}\left(\frac{\omega_{c,p}}{\omega}\right)\frac{(1-\omega/\omega_{c,p})^2}{(1-\omega/2\omega_{c,p})}\,\eta_p(v_{res})\,(A_p(v_{res})-A_c) \tag{12.28}$$

where $\eta_p(v_{res})$ and $A_p(v_{res})$ are the fraction number and anisotropy of the resonant ions and $A_c = (\omega_{c,p}/\omega - 1)^{-1}$ is the critical ion anisotropy for instability. When the convective properties of the ion-cyclotron waves are applied to the region of the Io plasma torus, one can define a critical ion flux for instability that is essentially identical to the electron-whistler value (12.24).

If the ion energy spectrum and pitch-angle anisotropy were known, predictions (analogous to Fig. 12.7) could be made for the unstable band of ion-cyclotron turbulence. The energetic ion spectrum in the middle magnetosphere, however, has been reported only at energies above 0.5 MeV (see Fig. 12.3). Nevertheless, the fluxes reported by Armstrong et al. [1981] near $L \approx 7.7$ are best modeled by an integral spectrum $J(>E_p) \approx 8 \times 10^{10}/E_p$ (MeV)/m^2-s-sr, so that all ions below $E_p \approx 1$ MeV would appear to have sufficient flux (12.24) to excite ion-cyclotron waves. This energy is substantially larger than $B^2/8\pi n \approx 10$ keV; one might therefore (in analogy with Fig. 12.7) anticipate a broadband of unstable waves resonant with 10 keV to 1 MeV ions. Unfortunately at $L = 7.7$ the predicted unstable band (1–5 Hz) occurs in a frequency range just below the lower limit of the plasma- wave instrument. But intense low-frequency electromagnetic waves could also be identified by the magnetometer on Voyager 1. To assess whether this is indeed feasible, we recall that limits on the wave amplitude can be obtained from the rate of pitch-angle scattering. The rapid depletion of the energetic ion flux inside $L \approx 8$ (Fig. 12.3) when compared to the expected rate of injection by interchange driven radial diffusion requires pitch-angle scattering near the strong diffusion rate (Fig. 12.2). If the scattering were indeed due to electromagnetic ion-cyclotron turbulence, it would require wave amplitudes $B' \gtrsim 1\ nT$ (Fig. 12.1). This should be within the resolution of the Voyager magnetometer [Acuña, private communication, 1980] but the anticipated scattering waves have not yet been reported.

Rapid ion scattering apparently occurs throughout the inner torus and by $L \approx 6$ the flux above 0.5 MeV has dropped by more than two orders of magnitude (Fig. 12.3) below the critical level J_p^* for ion-cyclotron instability. The persistent scattering loss of high-energy ions could, nevertheless, be maintained parasitically [as apparently also occurs for electrons with $E_e > 1$ MeV (see Fig. 12.6)] provided that lower energy ions (10–100 keV) remain available with adequate flux ($J_p > J_p^*$) to excite the plasma waves. Although this cannot be substantiated, it is entirely reasonable because the strong diffusion timescale for 10 keV ion removal is an order of magnitude longer than at 1 MeV (Fig. 12.2).

Low-frequency electrostatic waves offer an alternative mechanism for rapid ion removal from the inner torus. One potential wave mode is the electrostatic loss-cone instability [Post and Rosenbluth, 1966], which can lead to a broad band of unstable waves (centered just below the ion plasma frequency) in the high β magnetospheric environment [Coroniti, Fredericks, and White, 1972]. Plasma waves with the appropriate spectral properties have been detected beyond the terrestrial plasmapause [Anderson and Gurnett, 1973] and Scarf, Gurnett, and Kurth [1981] have reported broadband electrostatic noise bursts, which suggest that a modified version of this instability could be operative in the outer region of the Io plasma torus. However,

wave amplitudes near 10 mV/m are required to provide strong diffusion scattering of ions with $E_p \gtrsim 1$ MeV. Although this requirement appears to be larger than the observed wave intensities [Scarf, private communication, 1980], one cannot exclude such waves being the ion scattering mechanism owing to the limited spectral range of the plasma wave detector on Voyager.

The Voyager plasma-wave instrument also detected intense low frequency electric field noise near each crossing of the outer boundary of the Jovian plasma sheet [Barbosa et al., 1981]. As reported in Chapter 8, this emission is similar to the broadband electrostatic noise that is continuously present on auroral field lines in the terrestrial magnetosphere [Gurnett and Frank, 1977]. Potential candidates for this emission are electrostatic ion-cyclotron waves, excited either by the loss-cone instability or field-aligned currents [Ashour-Abdalla and Thorne, 1978] or lower-hybrid drift waves driven by perpendicular currents [Huba, Gladd, and Papadopoulos, 1978]. In either case, a significant Doppler shift would be required to explain the observed broadband spectrum. Analogous waves in the terrestrial environment adequately account for the observed strong diffusion scattering of ions ($E_p \lesssim 100$ keV) on auroral field lines and are thus thought to be the major mechanism for the diffuse proton aurora [Ashour-Abdalla and Thorne, 1978]. However, the wave amplitudes in the Jovian magnetosphere are significantly smaller (typically $\mathscr{E}' \sim 0.1$ mV/m; Fig. 8.20) and at best provide only weak diffusion. Such waves are certainly not responsible for the dramatic ion depletion inside $L \approx 8$.

Even though energetic ions in the middle Jovian magnetosphere may be subject to strong pitch-angle scattering, a comparison of the timescales for injection and removal (Fig. 12.2) indicates that the ion flux distribution $J(L)$ in the outer torus ($L \gtrsim 8$) is controlled by inward radial diffusive injection from the outer magnetosphere. Significant depletion by pitch-angle scattering and ultimate precipitation loss to the atmosphere occur only in the inner torus ($L \lesssim 8$). Within this loss dominated region, one can anticipate a reduction in the trapped flux to the critical level J_p^* appropriate for the excitation of either electromagnetic ion- cyclotron waves [Thorne and Coroniti, 1972] or the electrostatic loss-cone instability [Coroniti, Kennel, and Thorne, 1974]. Furthermore, high-energy ions may be scattered parasitically and thereby be reduced to flux levels well below J_p^*.

In an attempt to simulate the observed radial depletion in the phase-space density of energetic ions [Armstrong et al., 1981], one can solve the steady-state radial diffusion equation (12.18) under the assumption that losses approach the strong diffusion limit (12.9). The reported observations were for ions with a fixed magnetic moment, $\mu \approx 70$ MeV/G, for which the minimum lifetime is $\tau_{SD,p} = \tau_o L^{11/2}$ with $\tau_o \approx 1$ s for energetic protons. If the radial diffusion coefficient is modeled empirically by $D_{LL} = D_0 \mathrm{L}^m$, the diffusion equation (12.18) has an analytical solution [e.g., Irving and Mullineux, 1959 (see their Eq. 6.21)]

$$f_o(L_*) \sim L_*^{(m-3)/2}\,K_\nu(z) \tag{12.29}$$

where $K_\nu(z)$ is a modified Bessel function of the second kind of order $\nu = (2m\text{-}6)/(2m+7)$ and argument $z = L_*^{-(2m+7)/4}$ and

$$L_* = \left\{\left(\frac{2m+7}{4}\right)^2 D_o\tau_o\right\}^{2/2m+4} L \tag{12.30}$$

is a renormalized radial coordinate.

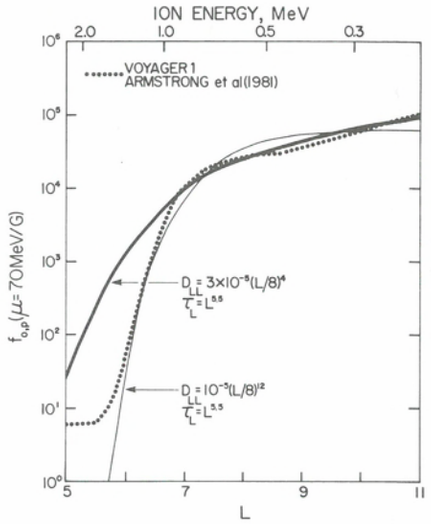

Fig. 12.11. The phase-space density of energetic (70 MeV/G) ions observed by Voyager 1 as a function of radial location. The dramatic decrease inside $L \approx 8$ has been modeled by balancing the rate of inward radial diffusion with strong diffusion precipitation loss. The best fit requires a change in the rate of diffusion inside $L = 8$ consistent with the models of centrifugally driven interchange instability recently proposed by Siscoe et al. [1981].

A comparison between the observed distribution function [Armstrong et al., 1981] and two theoretical solutions for different values of the radial diffusion index m is shown in Figure 12.11. Each theoretical solution is arbitrarily normalized, and the scaling coefficient D_o has been optimized to best simulate the radial gradient $\partial f/\partial L$ in the torus. As discussed by Siscoe, et al. [1981], radial diffusion with an index m $= 4$ is appropriate for centrifugally driven interchange instability in the outer ($L \geq 8$) region of the torus. This scaling was deduced from the observed radial gradient of outward diffusing thermal (40 eV) heavy ions. This same scaling with a similar magnitude D_o for the radial diffusion coefficient also provides an excellent fit (in the region $L \gtrsim 7$) to the radial profile for inward diffusing energetic ions subject to strong diffusion scattering loss. Inside $L \approx 8$, however, the strong radial gradient in the energy density (or pressure) of energetic ions can seriously inhibit the outward rate of diffusion of warm torus ions. The observed steep density gradient in the thermal ion distribution [Bagenal and Sullivan, 1980] near the outer edge ($L \approx 7.5$) of the UV emitting torus has been explained by Siscoe, et al. [1981] in terms of such a marked reduction in the rate of radial diffusion. They further suggest that a radial diffusion coefficient with an index $m = 12$ is appropriate for this region of the torus. This scaling has been adopted for the second theoretical solution shown in Figure 12.11, and it gives an excellent fit to the observed energetic ion distribution between $6 \lesssim L \lesssim 8$.

This result lends further support to the concept that radial diffusion driven in response to interchange instability of thermal torus ions is the major source for energetic plasma throughout the middle Jovian magnetosphere. It also provides compelling evidence that the energetic ions are indeed lost by precipitation into the Jovian atmosphere at a rate comparable to the limit imposed by strong pitch-angle diffusion. Although the precise mechanism for such scattering cannot be identified using available plasma-wave information from Voyager, the apparent absence of effective scattering loss inside $L \approx 5.5$ (Fig. 12.11) points towards the electromagnetic ion-cyclotron mode, which should be more easily excited in the high density torus. In the terrestrial magnetosphere such waves attain peak amplification well away from the equator [Joselyn and Lyons, 1976]. If this is also true for Jupiter, it might account for the absence of intense waves (with sufficient intensity to provide strong diffusion scattering) along the Voyager trajectory.

12.4. Precipitation fluxes and the Jovian aurora

Even before Voyager 1 entered the Jovian environment the extreme ultraviolet spectrometer made two important discoveries. The first were heavy ion (S^+, O^+, etc.) emission lines from a warm ($T_e \approx 10$ eV) dense ($n \approx 10^3/cm^3$) torus surrounding the orbit of Io, and the second were intense auroral HLyα and H_2 Lyman and Werner band emissions originating from the Jovian polar regions apparently mapping along field lines from the torus [Broadfoot et al., 1979]. The auroral emissions were particularly intense with a total radiated power of approximately 2×10^{12} W in HLyα and 3×10^{12} W in H_2 band emissions. Relevant cross-sections for auroral excitation by electron impact on H_2 have recently been measured by Yung et al. [1982] and the results have been employed to model the entire spectrum of auroral emissions from the Jovian atmosphere. They reported significant discrepancy with the excitation cross-sections published earlier by Stone and Zipf [1972], and, at the time of writing, these differences have not been reconciled. The best estimate to account for the total observed radiated power would require (0.3 to 1.2) $\times 10^{14}$ W to be dissipated by energetic electron precipitation. The quoted range reflects remaining uncertainties in the excitation cross-section and the problem of radiation extinction in the atmosphere. This required energy deposition is somewhat larger than the most recent value reported by Broadfoot et al. [1981], but it is comparable to the approximate estimates by Thorne [1981] based on the Lyα excitation cross-section computed by Miles, Thompson, and Green [1972].

From a detailed comparison of the color ratio in various wavelength ranges, Yung et al. [1982] also suggest a factor of two extinction in the emitted short wavelength radiation. This would place the required auroral energy input above 6×10^{13} W for electron impact with a typical precipitating electron energy near 10 keV. On the other hand, if ion precipitation were dominant, the auroral excitation would be due primarily to secondary electrons with a mean energy near 30 eV [Kuyatt and Jorgensen, 1963]. Because the efficiency for auroral excitation is considerably smaller for such electrons [Miles, Thompson, and Green, 1972] the required ion precipitation flux would exceed 10^{14} W [Thorne, 1981] and energies near 100 keV would be needed to account for the apparent atmospheric extinction at short wavelengths.

Although the energetic particle detectors on Voyager could not resolve fluxes within the atmospheric loss cone, an estimate for the average unidirectional precipitation flux inside the loss cone

$$j_P(E) = \frac{2}{\alpha_L^2} \int_0^{\alpha_L} j(E,\alpha) \sin\alpha \, d\alpha \tag{12.31}$$

can be obtained from the average directional trapped flux

$$j_T(E) = \int_{\alpha_L}^{\pi/2} j(E,\alpha) \sin\alpha \, d\alpha \tag{12.32}$$

and knowledge of the pitch-angle scattering lifetime [Coroniti and Kennel, 1970],

$$j_P(E)/j_T(E) \simeq \tau_{SD}(E)/\tau_L(E) \tag{12.33}$$

The precipitation flux is therefore always less than the averaged trapped flux, but the two become comparable under strong pitch-angle diffusion. Estimates for the particle lifetime obtained in Section 12.3 can thus be combined with information on the observed trapped fluxes to compute the net energy deposition into the Jovian atmosphere. Such estimates are given for each class of observed scattering wave turbulence,

and comparisons are made with the energy input required to account for the Jovian auroral luminosity.

The intense band of low frequency electromagnetic hiss observed throughout the Io plasma torus typically resonates with electrons above 100 keV. Near $L \approx 8$, the trapped energetic ($E_e \gtrsim 100$ keV) differential spectrum reported by Armstrong et al. [1981] can be modeled by the functional form

$$j\left(E_e, \alpha \approx \frac{\pi}{2}\right) \approx 3 \times 10^{13}/E_e^2(\text{keV})/\text{m}^2\text{-s-sr-keV} \tag{12.34}$$

For a pitch-angle distribution $j(E, \alpha) \sim \sin^2 \alpha$ the average trapped flux (12.32) is $j_T(E_e) \sim 2 \times 10^{13}/E_e^2/\text{m}^2\text{-s-sr-keV}$. The observed wave amplitude at this location provides scattering at a rate comparable to 5% of the strong diffusion limit (Fig. 12.10) which from (12.33) yields an average precipitation flux $j_P(E_e) \sim 10^{12}/E_e^2/\text{m}^2\text{-s-sr-keV}$. The net energy flux deposited into the Jovian atmosphere is therefore

$$\epsilon_P \approx \int E_e j_P(E_e)\, dE_e\, d\Omega \approx 2\pi 10^8\ \ell\text{n}\ (E_{\max}/E_{\min})\ \text{keV/cm}^2\,\text{s} \tag{12.35}$$

For resonant electrons in the range 150 keV $\lesssim E_e \lesssim$ 3 MeV (Fig. 12.10) the total precipitation energy flux due to scattering by electromagnetic hiss is $\epsilon_P \approx 3$ mW/m^2. Because the trapped electron flux exhibits relatively minor (less than a factor of 3) variability throughout the torus $6 \lesssim L \lesssim 10$ (Fig. 12.3) and because the rate of pitch-angle scattering at $L \approx 8$ is reasonably representative of average values throughout this region (see Fig. 12.8) one can anticipate an average energy deposition comparable to 3 mW/m^2 over an extended invariant latitude range $65° \lesssim \Lambda \lesssim 70°$ mapping from the torus. The total area of this extended diffuse auroral zone amounts to 2×10^{15} m^2 in both hemispheres. Total power dissipated by the energetic ($\gtrsim$ 150 keV) electron precipitation is therefore approximately 6×10^{12} W, as initially established by Thorne and Tsurutani [1979]. Although such intense precipitation constitutes a major energy source for the Jovian ionosphere, it is substantially less than the input required to explain the observed auroral emissions. Furthermore, even if the energetic electrons were scattered near the strong diffusion rate, the energy deposition would occur deep in the atmosphere where short wavelength extinction is catastrophic [Yung et al., 1982]. One must therefore look for an alternative source for the Jovian aurora.

The role played by electromagnetic chorus emissions, which predominantly resonate with electrons near 1 keV was initially considered by Coroniti et al. [1980]. Observational data on the resonant electron flux were unavailable at the time of their analysis, and the computed ($E_e \approx$ keV) energy deposition was therefore based purely on theoretical considerations. The distribution function of electrons below 6 keV has now been reported by Scudder, Sittler, and Bridge [1981a], and one can therefore make a more realistic assessment of the low energy precipitation flux. Over the relevant energy range, 300 eV $\lesssim E_e \lesssim$ 4 keV, the electron differential flux near $L \approx 8$ is best fit by the spectrum

$$j\left(E_e, \frac{\pi}{2}\right) \approx 10^{12}/E_e(\text{keV})/\text{m}^2\text{-s-sr-keV} \tag{12.36}$$

To excite chorus at frequencies above $f_{ce}/2$, the resonant electrons must be highly anisotropic ($A_e \gtrsim 1$). Because observational information is unavailable, we optimistically assume a pitch-angle distribution $j(E_e,\alpha) \sim \sin^4 \alpha$ that yields an average trapped flux $j_T(E_e) \sim 5 \times 10^{11}/E_e/\text{m}^2\text{-s-sr-keV}$. The intensity of chorus emissions observed near

$L \approx 8$ provides scattering of 2–4 keV electrons within a factor of two of the strong diffusion rate (Fig. 12.10). The average precipitation flux is therefore $j_P(E_e) \approx 2.5 \times 10^{11}/E_e/\text{m}^2\text{-s-sr-keV}$, and the net energy deposition into the atmosphere is

$$\epsilon_P(2\ \text{keV} \lesssim E_e \lesssim 4\ \text{keV}) \approx 0.5\ \text{mW/m}^2 \tag{12.37}$$

This is substantially smaller than the total precipitation energy flux of higher energy electrons scattered by hiss. Also, even if chorus were continually present throughout the torus (which apparently is not the case), the total power dissipation by the resonant low-energy electrons would be less that 10^{12} W. Scattering by chorus therefore plays a relatively minor role in Jovian auroral energetics.

The importance of the third class of wave capable of causing electron precipitation, namely the electrostatic $(n + 1/2)$ cyclotron harmonic waves, has not previously been considered in the auroral context. The waves are continuously present near the equatorial plane in the outer torus and predominantly resonate with lower energy electrons. Estimates for the precipitation lifetime near $L \approx 8$ are illustrated in Figure 12.10. Observed wide-band wave amplitudes near $L \approx 8$ ($\mathscr{E}' \sim 0.1$ mV/m) can provide strong diffusion scattering at $E_e \approx 100$ eV, but the scattering becomes progressively weaker at higher energy. Using (12.27) for the resonant electron lifetime and (12.36) for the trapped electron flux, one obtains an average precipitation flux

$$j_P(E_e) \approx 5 \times 10^9/E_e^3\ (\text{keV})/\text{m}^2\text{-s-sr-keV} \tag{12.38}$$

and a net energy deposition $\epsilon_P(E_e > 300\ \text{eV}) \approx 2 \times 10^{-2}$ mW/m^2. This is substantially smaller than the contribution by either chorus or hiss. Thus, even if the electrostatic wave amplitudes attain their peak value near 1 mV/m [Kurth et al., 1980b] the net energy deposition flux would only approach $\epsilon_p(E_e > 1\ \text{keV}) \sim 0.5$ mW/m^2 and the total power dissipation over the entire latitude range mapping from the torus would amount to less than 10^{12} W. Electrostatic waves are therefore unable to significantly contribute to the auroral deposition mechanism.

Because the most liberal estimates for overall electron energy deposition into the Jovian atmosphere ($\lesssim 10^{13}$ W) fall short of the required auroral input, one must turn to energetic ion precipitation as an alternative mechanism. Unfortunately, our ability to quantitatively model the ion input has a weaker observational basis. Although there is compelling evidence for strong diffusion scattering loss of energetic ions in the torus, the scattering mechanism cannot be established, and the trapped ion flux has only been reported for energies above 500 keV. Nevertheless, in the central region of the torus ($L \sim 7.7$) the trapped ion flux between 500 keV and 2 MeV [Armstrong et al., 1981], can be represented by the spectrum

$$j\left(E_p, \frac{\pi}{2}\right) \approx 7 \times 10^{13}/E_p^2(\text{keV})/\text{m}^2\text{-s-sr-keV} \tag{12.39}$$

The ion pitch-angle distribution varies as $j(E_p,\alpha) \sim \sin^2 \alpha$ [Lanzerotti et al., 1981], which yields an average trapped flux $j_T(E_p) \sim 5 \times 10^{13}/E_p^2/\text{m}^2\text{-s-sr-keV}$. In the absence of any information on the scattering waves, one can simply resort to the excellent fit to the radial diffusion profile (Fig. 12.11) and infer that ions are indeed scattered at a rate comparable to strong pitch-angle diffusion. Conservatively, we may assume scattering at 30% of the strong-diffusion limit and take an average precipitation flux $j_P(E_p) \sim 0.3\, j_T(E_p)$. This provides an energy deposition flux

$$\epsilon_P(E_{\min} \lesssim E_p \lesssim E_{\max}) \approx 10^{14}\ \ell\text{n}\ (E_{\max}/E_{\min})\ \text{keV/m}^2\text{-s} \tag{12.40}$$

Because the ions are subject to such rapid scattering loss, intense precipitation is limited to a relatively narrow range of invariant latitude $67° \leq \Lambda \leq 70°$ mapping from the middle torus $7 \leq L \leq 9$ (see Fig. 12.11); namely over an area $\approx 10^{15}$ m^2 in both hemispheres. The total power dissipation is therefore $\approx 1.5 \times 10^{13} \ln (E_{max}/E_{min})$ W. Over the observed energy range (0.5 MeV $\leq E_p \leq$ 2.0 MeV), the anticipated power dissipation should be approximately 2×10^{13} W in rough agreement with the earlier estimate by Goertz [1980b]. Although this is still below the input required to excite the observed aurora, an extrapolation of the measured trapped ion spectrum (12.39) to energies below 100 keV enhances the total power dissipation to values comparable to the anticipated auroral requirements $\approx 10^{14}$ W. Furthermore, in contrast to the energetic electron precipitation, ions will deposit their energy in the higher altitude region of the Jovian atmosphere where extinction of auroral emissions is relatively unimportant. Precipitating ions in the energy range near 100 keV should therefore be considered the leading candidate for excitation of the diffuse Jovian aurora.

12.5. Energy transfer processes

Although the energy flux of plasma waves in the Jovian magnetosphere is miniscule in comparison to the observed energy flux in trapped radiation belt particles (see Table 12.2), the ability to efficiently scatter resonant particles in velocity space can cause rapid particle loss and significant energy deposition into the Jovian atmosphere. The most intense particle precipitation is anticipated over a relatively broad range of invariant latitudes mapping from the high density plasma torus surrounding the orbit of Io. The Jovian aurora should therefore be predominantly diffuse in nature, in contrast to the Earth where the most intense energy deposition occurs in discrete auroral arcs. A second major distinction between the Jovian and terrestrial aurora is that energetic ions probably provide the major energy input at Jupiter. Estimates based on the observed trapped-particle flux and the intensity of plasma waves in the Jovian magnetosphere indicates that the total power dissipation by low energy ($\sim$ few keV) precipitating electrons should barely exceed 10^{12} W (Sec. 12.4). In analogy with the terrestrial aurora the energy deposition could be enhanced by invoking a field aligned potential difference between the magnetosphere and the atmosphere but this would have to exceed several tens of keV over an extended range of L to account for the observed auroral emissions. More energetic electrons ($>$ 100 keV) may dissipate up to 10^{13} W, but the energy deposition occurs so deep in the atmosphere that most of the resulting auroral emissions would be reabsorbed. It therefore appears that ion precipitation near the limit imposed by strong diffusion offers the only viable mechanism to account for the observed auroral emissions. Unfortunately, although there is compelling evidence for rapid loss of energetic ($>$ 500 keV) ions from the region of the torus, lower energy ions, which should contribute most of the energy deposition, were not detected in the inner magnetosphere by Voyager 1. Furthermore, the precise mechanism for strong diffusion scattering cannot be established owing to the absence of plasma-wave observations in the appropriate resonant frequency range. These deficiencies should be remedied by instrumentation carried on the future Galileo mission.

The enormous power that is continuously dissipated in the Jovian auroral zone places stringent limits on the mechanisms responsible for injecting energy into the magnetosphere. As an example, the total power available from the solar wind incident over the entire Jovian magnetosphere is approximately 10^{15} W. If this were to provide the ultimate source for auroral dissipation, the energy transfer mechanism would have to be far more efficient (namely 10%) than the analogous processes at Earth. It is

Table 12.2. *Wave-particle energetics in the Jovian magnetosphere*

Wave mode	Amplitude	E_{res}	Energy flux (mW/m^2) Waves	$\epsilon_T(E_{res})$	$\epsilon_p(E_{res})$
Whistler-mode hiss	$B' \sim 30$ mγ	$E_e \gtrsim 100$ keV	2×10^{-6}	60	3
Chorus	$B' \sim 10$ mγ	$E_e \sim$ few keV	10^{-6}	1	0.5
Electrostatic electron cyclotron	$\mathscr{E}' \sim 1$ mV/m	$E_e \sim$ (1-10) keV	2×10^{-8}	3	0.5
Electromagnetic ion-cyclotron	$B' \sim 1\gamma$	$E_p \gtrsim 10$ keV	2×10^{-4}	200	70

therefore unlikely that the solar wind contributes significantly to the energetics of the Jovian magnetosphere. The rapid rotation of Jupiter, however, has the potential of providing significant power input to the magnetosphere [e.g., Gold, 1976; Carbary, Hill, and Dessler, 1976]. One specific mechanism for tapping this rotational energy is through the torque exerted by Jupiter on the heavy ions injected into the torus surrounding the orbit of Io [e.g., Dessler, 1980b]. The total power input is proportional to the rate of ion injection. Half of this power is consumed in driving bulk motion of the plasma and the remainder represents an upper limit on the power available for auroral dissipation [Eviatar and Siscoe, 1980]. The inferred aurora input of approximately 10^{14} W therefore places a lower bound on the rate of ion production in the torus $dM/dt \gtrsim 2 \times 10^{30}$ amu/s or roughly 10^{29} ions s^{-1} if we adopt $A_+ \approx 25$ for the mean atomic mass of heavy ions in the torus [Bagenal and Sullivan, 1981]. For the reported total torus population of 5×10^{34} ions [Bagenal and Sullivan, 1981] the mean residence time in the torus would be approximately 7 days, which is not inconsistent with the rapid rate of interchange driven radial diffusion computed by Siscoe et al. [1981] (also see Fig. 12.2) or the convection time estimated by Hill, Dessler, and Maher [1981].

It should be emphasized, however, that such rapid mass loading and short residence times in the torus are not universally accepted. On the assumption that most of the neutral atoms are ionized within 1 R_J of Io, Shemansky [1980b] concludes that the absence of detectable UV emissions near Io limits the ion production to values near 10^{27} ions s^{-1}. Such a low mass loading, however, would provide little more than 10^{12} W to the magnetosphere. This would barely be sufficient to balance the radiative cooling of the torus (the total power in UV emission is approximately 2.5×10^{12} W [Sandel et al., 1979]) and would be totally inadequate to drive the more intense and continuous auroral dissipation. One must therefore conclude that if mass loading is indeed the ultimate energy source for energizing the magnetosphere and subsequently exciting the aurora, the neutrals released from Io must either be ionized over a more extended region, or the initially produced ions species must be of a form that cannot be detected by the extreme ultraviolet spectrometer (e.g., SO_2^+).

A further consequence of the rapid mass loading is that the cold electrons ($T_- \approx 10^{-2}$ eV) and the warm ($T_+ \gtrsim 300$ eV) heavy ions initially produced in the corotating torus cannot equilibrate by direct Coulomb energy transfer which requires a time [Spitzer, 1962].

$$\tau_{\pm} \sim \frac{3 \times 10^5 A_+ A_e}{z_+^2 n_e} \left\{ \frac{T_+}{A_+} + \frac{T_e}{A_e} \right\}^{3/2} \tag{12.41}$$

where $A_{\pm}$ are the ion and electron mass in amu, $T_{\pm}$ are the ion and electron temperatures in eV, and n_e is the electron number density. Adopting average properties for plasma observed in the torus $A_+ \sim 25, Z_+ \sim 1.5, n_e \sim 10^3/\text{cm}^3, T_e \sim 10$ eV [Bagenal and Sullivan, 1981; Scudder, Sittler, and Bridge, 1981a] one obtains a Coulomb energy transfer time $\tau_c \approx 5 \times 10^6$ s, which is longer than any realistic residence time. Furthermore, the total power input to the electron gas due to Coulomb interaction with heavy ions, is $n_+ T_+ V/\tau_c$ where $V \approx 5 \times 10^{25}$ m^3 is the effective volume of the radiating torus. For the observed mean ion energy, $T_+ \sim 40$ eV, this provides a total power supply $\approx 5 \times 10^{10}$ W. Because of the sensitivity of these estimates to the average electron density and temperature in the torus, neither of which are precisely known, Brown [1982] has suggested that the rate of energy transfer could be considerably larger. But even with the most optimistic choice of plasma parameters, the rate of electron heating is below the known radiative-cooling rate ($\sim 3 \times 10^{12}$ W) of the torus. One must therefore look for an alternative source to maintain the torus electrons above the temperature ($\gtrsim 10$ eV) required to excite the observed UV emissions.

An important clue to the nature of this heat source has recently been provided by Scudder, Sittler, and Bridge [1981a] who reported a bimodal electron distribution in the outer torus. Near $L \approx 8$, the dense Maxwellian population, with $T_e \sim 20$ eV, is found in conjunction with a suprathermal tail (containing comparable energy flux) extending to energies above several keV. Because the time-scale for energy equilibration between hot and cold electrons is substantially shorter than between electrons and heavy ions, these suprathermal electrons could provide a viable heat source for the torus. For example $\lesssim 100$ eV suprathermal electrons will equilibrate with the cold torus electrons within a few hours.

One possible source for these suprathermal electrons in the magnetosphere are secondary electrons produced during the intense ion precipitation into the Jovian atmosphere. The average energy of secondary electrons emitted during the energetic proton impact on H_2 is typically 20 to 40 eV [Kuyatt and Jorgensen, 1963; Rudd, Sautter, and Bailey, 1966] but a significant number can also be produced with energies up to several keV. Those produced in the upward hemisphere above an altitude where the mean free path exceeds the amospheric scale height, can escape into the magnetosphere with little energy loss. The differential flux of escaping secondaries with energy E has recently been computed by Thorne [1981],

$$j(E) \simeq [\tilde{\sigma}_s(\text{E})/\sigma_{\text{ion}}(E)]\, J_P(> E_{+,\text{min}}) \tag{12.42}$$

where $\tilde{\sigma}_s(E)$ is the average differential cross-section for secondary electron production, $\sigma_{\text{ion}}(E)$ is the electron ionization cross-section and J_P is the integral flux of precipitation ions above the minimum energy $E_{+,\text{min}} \approx (E + 15.6\text{ eV})\, M_+/4\text{m}_-$ required for secondary electron production in H_2 where the ionization potential is 15.6 eV. Using the experimentally determined cross-sections and adopting an average precipitation ion flux $J_P(> E_p) \approx 10^{14}/E_p(\text{keV})/\text{m}^2\text{-s}$ as deduced in Section 12.4, one can integrate (12.42) to obtain both the net integral flux in escaping secondary electrons and the heat flux into the magnetosphere. Note that to escape from the atmosphere the secondary electrons must carry with them an equal flux of cold ionosphere H^+ ions; this is possible because their energy exceeds the gravitational potential (≈ 10 eV) for ambipolar outflow from the Jovian atmosphere [Ioannidis and Brice, 1971].

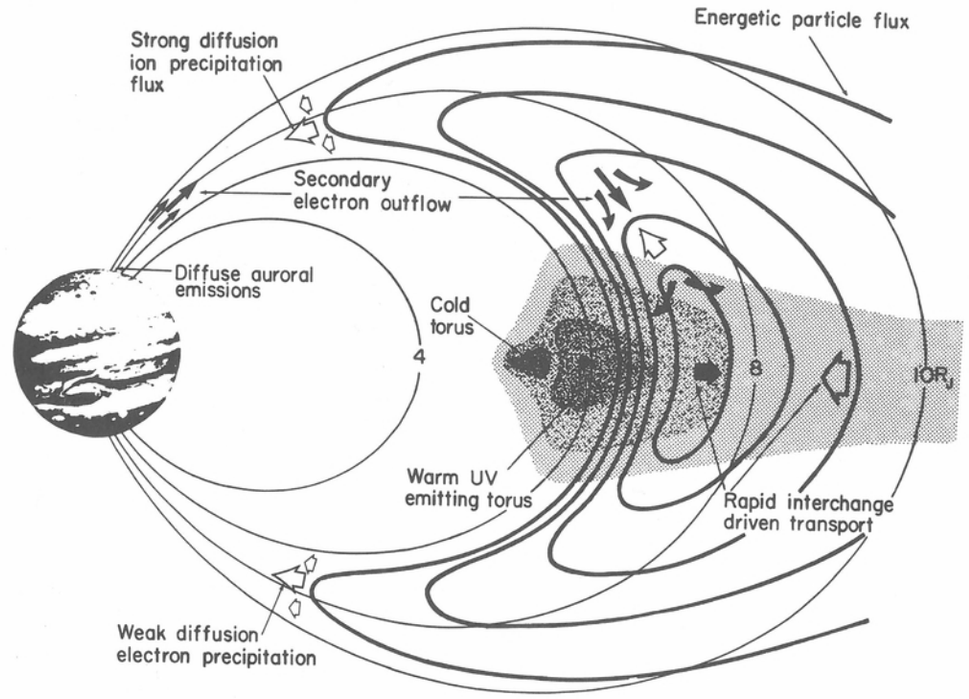

Fig. 12.12. A schematic view of physical processes associated with the heavy ion torus (shaded) surrounding Io. The flux of energetic ring current ions exhibits a steep inner edge near $L \approx 7$, presumably owing to strong diffusion precipitation. Energetic ion precipitation leads to the outflow of superthermal secondary electrons and cold H^+ from the Jovian auroral zone. The upflowing ionospheric particles are scattered onto magnetospherically trapped orbits during their initial transit through the outer torus and subsequently redistributed in radius by eddies associated with interchange instability of the heavy ions injected by Io.

If energetic proton precipitation predominates, the anticipated heat flux to the magnetosphere from the entire auroral zone should amount to approximately 3×10^{11} W and cold H^+ ions would be injected into the torus at a rate comparable to 10^{28} ions/s. However, if the auroral precipitation is dominated by heavy ions (S^+ or O^+), the energy dissipation occurs higher in the atmosphere, $\tilde{\sigma}_s$ will typically be larger by the ratio M_+/M_p, and a larger fraction of the secondary electrons produced in the atmosphere can escape. The heat flux to the magnetosphere could then exceed 10^{12} W and cold H^+ ions would be injected into the torus at a rate on the order of 2×10^{29} s which is comparable to the most optimistic estimates for heavy ion injection from Io. A schematic view of this coupling between the auroral zone and the torus is illustrated in Figure 12.12.

Eviatar, et al. [1982] have considered the implications of such a substantial ionospheric input. The combination of the direct electron heat flux and the more rapid Coulomb energy transfer from heavy ions due to the substantial H^+ concentrations can account for both the apparent cooling of the heavy ions to the observed temperatures near 40 eV and the maintenance of the electron temperature above 10 eV. Because of the ambipolar electric fields, the peak H^+ ion concentrations are expected

well away from the equatorial plane in a region not explored by Voyager. This conclusion is supported by whistler dispersion observations [Gurnett et al., 1981b] which require substantially more columnar electron density than can be accounted for by heavy ions in the equatorial torus. Furthermore, although the plasma science instrument on the Voyager spacecraft could not directly detect thermal H^+ ions in the inner torus, significant H^+ concentrations ($\approx$ 30%) have been reported by McNutt, Belcher, and Bridge [1981] in the middle magnetosphere ($L \gtrsim 10$), and Hamilton et al. [1980] have discovered energetic H_3^+ and H_2^+ ions in the outer Jovian magnetosphere. Both observations suggest that the ionosphere is an important plasma source.

The injected ionospheric plasma should be rapidly scattered onto trapped orbits in the magnetosphere during the initial transit of the high density plasma torus and subsequently redistributed in radial location by the eddies associated with interchange instability of the heavy ions injected from Io or by corotating magnetospheric convection [e.g., Hill, Dessler, and Maher, 1981]. However, the outward flow of thermal heavy ions exhibits no evidence for systematic adiabatic cooling. Some additional heat input is therefore required to maintain the ion temperatures near 100 eV. Plasma waves or secondary-electron heat flux from the extended Jovian aurora zone are potential candidates. An important implication of the high thermal ion temperatures in the outer magnetosphere is that subsequent inward transport leads to adiabatic heating to energies comparable to 100 keV in the region of the torus. Rapid inward radial transport can therefore provide a means of maintaining the energy content of the Jovian ring current plasma, which is the reservoir for auroral dissipation. Whether this transport is dominated by interchange eddies, corotating magnetospheric convection or other processes remains to be determined.

ACKNOWLEDGMENTS

The author wishes to thank F. V. Coroniti, A. J. Dessler, A. Eviatar, D. A. Gurnett, F. L. Scarf, M. Schulz, G. L. Siscoe, B. T. Tsurutani, and Y. L. Yung for advice and constructive criticism during the preparation of this report. S. R. Church computed the Bessel functions used in the ion radial diffusion solution. The work was supported in part by N.S.F. Grants ATM 81-10517 and ATM 81-19544.

APPENDIX A
SYMBOLS AND ACRONYMS

Symbols

A — amps
collecting area of telescope
angstroms
atomic mass number
A_+ mean atomic number of ions

$\tilde{\mathbf{A}}$ — magnetic vector potential

A_p — geomagnetic index

A_0 — spin averaged flux
A_1 — first order anisotropy in particle flux
A_2 — second order anisotropy in particle flux
A_n — n^{th} order anisotropy in particle flux

A_c — critical anisotropy of electrons required for instability
A_e — pitch angle anisotropy of resonant e^-

B — magnetic field
- B_r, B_θ, B_ϕ — right-hand spherical components of **B**
- B_ρ, B_ϕ, B_z — right-hand cylindrical components of **B**
- B_A — magnetic field (strength) at the top of the atmosphere
- B_c — projection of **B** onto Jovigraphic equatorial plane
- B_{eq} — equatorial magnetic field
- B_I — magnetic field at Io
- B_{max} — maximum hourly average magnetic field
- B_T — magnetic field in tail lobes
- $\mathbf{B}_0$ — background magnetic field
- $\hat{\mathbf{B}}$ — unit magnetic field vector
- $\hat{\mathbf{B}}\hat{\mathbf{B}}$ — unit dyadic of magnetic field

b — any magnetic field external to the current sheet, other than the planetary dipole and the planar field of the current sheet itself

$\hat{\mathbf{b}}$ — unit vector parallel to **b**

c — speed of light

D — dispersion (units s-$Hz^{1/2}$)